Bull. Min. Res. Exp. (2021) 166: 85-112

Bulletin of the Mineral Research and Exploration

http://bulletin.mta.gov.tr

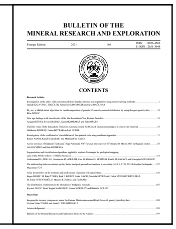

Active tectonics of Gülpınar-Tuzla area (Biga Peninsula, NW Turkey): the source of 6 February-24 March 2017 earthquake cluster

Ali KOÇYİĞİT[a] and Şule GÜRBOĞA[b*]

[a]Middle East Technical University, Department of Geological Engineering, Active Tectonics and Earthquake Research Laboratory, Ankara, Turkey

[b]General Directorate of Mineral Research and Exploration, Department of Geological Research, Ankara, Turkey

Research Article

Keywords:
Active Tectonics, Recent Seismicity, Southern Major Strand, NAFS, Biga Peninsula.

Received Date: 06.08.2020
Accepted Date: 19.08.2021

ABSTRACT

The variation in the motion sense of Anatolian platelet in Aegean Sea resulted in a strike-slip tectonic regime and related neotectonic domain, the central to northern Aegean neotectonic province, which also includes both western Marmara Sea and Biga Peninsula. Our study focuses mostly on the Gülpınar-Tuzla earthquake area located at the southwestern tip of Biga Peninsula, which is controlled by the southern major strand of the North Anatolian Fault System (NAFS). The strand consists of two sections, the onshore Biga and offshore Babakale-Skyros sections. Both sections are seismically very active. The Gülpınar-Tuzla earthquake area is composed of the Paleozoic metamorphic rocks, the Oligo-Miocene granitoid pluton, Lower-Middle Miocene calc-alkalic volcanic rocks and the Upper Miocene-Pliocene sedimentary sequence. All of these rocks, which formed and deformed (folded to tilted) in palaeotectonic period, are overlain with an angular unconformity by the Quaternary neotectonic basin fill, that is nearly flat-lying except for the faulted basin margins. Both the onshore and offshore sections of the southern strand are linked to each other in terms of the structures characterizing the Babakale pull-apart basin and the Gülpınar-Tuzla earthquake area. The latter is shaped by the NE-trending Gülpınar (GFZ) and Yenice-Gönen Fault Zone (YGFZ), the ENE-trending Edremit fault zone (EFZ), the WNW-trending Tuzla Fault Zone (TFZ) and three strike-slip basins (Ayvacık, Behramkale and Tuzla basins) developed along them. Some segments of both the TFZ and GFZ were reactivated by the occurrences of seven moderate-to small-sized independent earthquakes and related aftershocks over 2760. Five of the independent earthquakes have an origin of oblique-slip normal faulting, while the rest two seismic events are strike-slip faulting in origin. Focal mechanism solution diagrams of these two groups of earthquakes reveal that the Gülpınar-Tuzla area is under the control of a strike-slip neotectonic regime, which commenced in Early Quaternary time owing to the major inversion in extensional palaeotectonic regime. This is also supported by the palaeostress analysis of slip-plane data measured on fault slickensides. The uniform slip rates on both the YGFZ and EFZ are 10.8 mm/yr and 7.3 mm/yr, respectively.

1. Introduction

There is a close relationship between the plate tectonic configuration of Turkey and the current neotectonic regimes operating across it. From the palate tectonic point of view, Turkey and its near vicinity are shaped by several plates such as the African, Arabian, Eurasian and Anatolian plates, and their boundary fault systems of dissimilar character

Citation Info: Koçyiğit, A., Gürboğa, Ş. 2021. Active tectonics of Gülpinar - Tuzla area (Biga peninsula, NW Turkey): the source of 6th February - 24th March 2017 earthquake cluster. Bulletin of the Mineral Research and Exploration 166, 85-112. https://doi.org/10.19111/bulletinofmre.984922

*Corresponding author: Şule GÜRBOĞA, sule.gurboga@gmail.com

(Figure 1a). Major plate boundaries are the South Aegean-western Cyprian convergent plate boundary or subduction zone, the sinistral Dead Sea, East Anatolian and the dextral North Anatolian Fault systems. NAFS is in the nature of intra-continental transform fault. It accommodates the westward relative motion of the southerly located Anatolian Platelet. In the Aegean Sea, the Anatolian platelet and its westward motion are blocked and forced to move in south-southwest direction by a barrier, the mainland Greece (Şengör, 1980). This process results in a principal compressive stress. It operates in approximately E-W direction across the northern to central Aegean Sea and northwestern Anatolia. Thus, the bifurcation of the NAFS into two major fault strands around Sea of Marmara, their bending at ~30° towards south in just west of the imaginary Bandırma-Tekirdağ line (Figure 1b), and blocking and forcing of the Anatolian platelet to move southwestwards altogether change the architecture of the westernmost section of the NAFS, and leads to the emergence of a new neotectonic regime and province, namely the central to northern Aegean neotectonic province. It is characterized by the strike-slip neotectonic regime. The eastern boundary of this neotectonic province is the Balıkesir-İzmir fault zone (BİFZ) (Koçyiğit, 2020) (Figure 1a). This mega shear zone was previously named as the İzmir-Balıkesir Transfer Zone by Sözbilir et al. (2013). This neotectonic province includes western Marmara Sea, Biga Peninsula, and central to northern Aegean seas (Figure 1b). In this neotectonic domain both major strands of the NAFS are seismically very active. It is indicated by a series of destructive big earthquakes occurred in them (Ambraseys, 1988; Kiratzi et al., 1991; Papazachos et al., 1991; Taymaz et al., 1991; Ambraseys and Jackson, 1998; Papazachos et al., 1998; Papazachos, 2003; Tan et al., 2008; Aksoy et al,. 2010; Karakaisis et al., 2010; Kürçer et al., 2015) (Table 1). The eastern half of the southern strand trends in approximately E-W direction and follows the southern coastal area of Marmara Sea up to Lakes Ulubat-Manyas and Edincik areas, where it bends south at different angles (30°-60°) and then forms the structurally very complicated Biga section of the southern strand. In general, the Biga section trends in SW direction and consists of, from NW to SE, the Çan-Biga, Sarıköy-Inova, Bayramiç-Ezine, Yenice-Gönen, Balıkesir-İzmir, Ilıca-Darıca, Havran-Danişment, and the Edremit fault zones (Figure 1b). These fault zones first combine with the E-W trending Edremit fault zone and then are linked with the offshore Babakale-Skyros fault zone in terms of the intervening oblique-slip normal faults and related strike-slip basins such as the Balıkesir, Edremit Gulf, Ayvacık, Tuzla, Babakale (Bababurnu) and Skyros basins (Figure 1b) (Eryılmaz and Yücesoy, 1999; Koukouvelas and Aydın, 2002). Both the Babakale-Edremit gulf basins and their margin boundary faults were previously studied and reported (Güney et al., 2001; Beccaletto and Steiner, 2005; Yaltırak et al., 2013; Sözbilir et al., 2016). The remaining Çan-Biga, Sarıköy-Inova, Bayramiç-Ezine, Yenice-Gönen, Havran-Danişment, Ilıca-Darıca and the Balıkesir-İzmir fault zones were also studied in detail and mapped on 1/25.000 scale by authors of the present paper. However, except for their key sections (inserts in the Figure 1b), their descriptions are outside the present paper owing to avoid of increasing the volume of present manuscript.

Basic problems in the central to northern Aegen neotectonic province are: 1) type and onset age of the neotectonic regime, 2) total displacement and slip rates on fault zones, and 3) confusion of neotectoctonic strike-slip basins with the grabens of palaeotectonic origin. These points are still under debate, i.e., there is no a common agreement among researchers on these points (Herece, 1990; Karacık and Yılmaz, 1998; Yılmaz et al., 2000; Güney et al., 2001; Yılmaz and Karacık, 2001; Beccaletto and Steiner, 2005; Kürçer et al., 2008; Emre and Doğan, 2010). The present paper introduces some key structures comprising the southwesternmost tip of the Biga Peninsula. This area was also previously studied and interpreted as graben and horst originated from N-S extension (Yılmaz and Karacık, 2001). Whereas our recent studies based on detailed field geological mapping indicated that this area is under the control of a strike-slip neotectonic regime governed by a major principal compressive stress operating in approximately WNW direction. The Behramkale-Babakale, Gülpınar and Tuzla areas, which comprise the southwest onshore tip of Biga Peninsula, have a very significant linkage role between offshore (the Babakale-Skyros fault zone) and onshore (Yenice-Gönen fault zone) sections of the southern strand of the NAFS (Figure 1b). Consequently, the present paper has two basic goals: 1) to evaluate the major inversion in earlier extensional palaeotectonic regime, and commencement age of the strike-slip neotectonic regime, and 2) to describe both the active tectonics and related very recent seismic activity (the

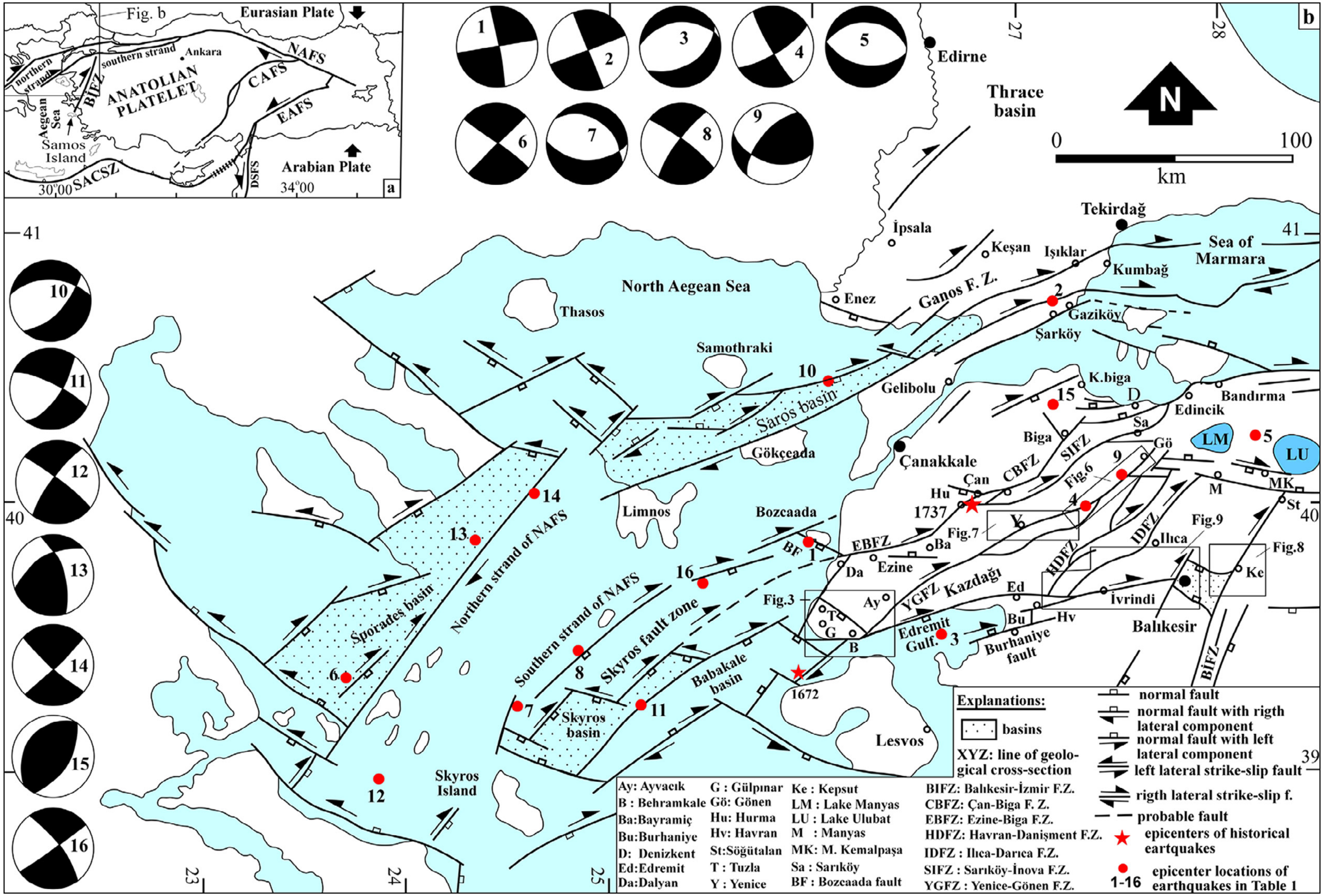

Figure 1- a) Simplified map showing major fault systems in Turkey and adjacent areas. BİFZ: Balıkesir-İzmir fault zone, CAFS: Central Anatolian Fault System, DSFS: Dead Sea Fault System, EAFS: East Anatolian Fault System, NAFS: North Anatolian Fault System, and SACSZ: South Aegean-Cyprus subduction zone, b) simplified seismotectonic map showing both the northern and southern major strands of the North Anatolian Fault Systems, epicenters of destructive earthquakes occurred in them and the location of the study area. EFZ: Edremit fault zone; GFZ: Gülpınar fault zone, and TFZ: Tuzla fault zone (offshore sections of faults and basins were modified from Koukouvelas and Aydın, 2002).

Table 1- Significant destructive earthquakes occurred within both the northern and southern major strands of the North Anatolian Fault System.

No	Date	Origin time	Epicentral coordinate		Depth (km)	Magnitude	Nodal plane 1			Nodel plane 2			References
			Northing	Easting			strike	dip	rake	strike	dip	rake	
1	1672.02.14	--	39.8	26.0	5-15	Mw=7.0	260	90	177	--	--	--	Papazachos, 2003; Karakaisis et al., 2010
2	1912.08.09	01:29	40.7	27.2	16	Ms=7.4	68	55	-145	--	--	--	Aksoy et al., 2010; Ambraseys and Jackson 1998; Kalafat et al., 2011
3	1944.10.06	02:34	39.48	26.56	40	Ms=6.8	--	--	--	--	--	--	Ambraseys, 1988; Kalafat et al., 2011; Papazachos et al., 1991
4	1953.03.18	19:06:13	40.0	27.30	5-15	Ms=7.4	150	84	14	59	76	174	Tan et al., 2008
5	1964.10.06	14:31:23	40.3	28.2	5-15	Ms=6.9	273	46	-95	101	44	-87	Papazachos et al., 1991
6	1965.03.09	17:57:54	39.3	23.8	5-15	Ms=6.1	40	90	-6	310	86	-180	Papazachos et al., 1991
7	1967.03.04	17:58:09	39.2	24.6	8	Ms=6.6	98	54	-107	302	42	-70	Kiratzi et al., 1991
8	1968.02.19	22:45:42	39.4	24.9	9	Ms=7.1	217	86	175	310	82	4	Kiratzi et al., 1991
9	1969.03.03	00:59:10	40.1	27.5	6	Ms=6.0	221	64	41	112	54	149	Tan et al., 2008
10	1975.03.27	05:15:08	40.4	26.1	15	Ms=6.6	41	60	-128	279	46	-42	Papazachos et al.,1991
11	1981.12.19	14:10:51	39.2	25.2	8	Ms=7.2	37	67	-166	303	77	-22	Tan et al., 2008
12	1981.12.27	17:39:13	38.9	24.9	8	Ms=6.5	212	85	-174	123	84	-66	Taymaz et al., 1991
13	1982.01.18	19:27:25	39.8	24.4	9	Ms=7.0	235	50	153	343	70	43	Tan et al., 2008
14	1983.08.06	15:43:52	40.0	24.7	8	Ms=6.8	48	83	178	136	88	07	Papazachos, 2003; Karakaisis et al., 2010
15	1983.07.05	12:01:27	40.3	27.2	10	Ms=6.1	248	70	-155	149	66	-22	Harvard GCMT catalogue
16	2013.01.08	14:16:07	39.64	25.48	8	Mw=5.7	54	89	-166	--	--	--	Kürçer et al., 2015

6 February-24 March 2017 Gülpınar-Tuzla eartquakes cluster) occurred at the tip of Biga Peninsula under the light of our field data and the international literature including mostly submarine geophysical studies and related seismic data (Eryılmaz and Yücesoy, 1999; Güney et al., 2001; Koukouvelas and Aydın, 2002; Beccaletto and Steiner, 2005; Kurtuluş et al., 2009; Yaltırak et al., 2013; Sözbilir et al., 2016). Thus, we aim to contribute to the solution of abovementioned basic problems. In addition, in the present paper the term “earthquake cluster” was used in the meaning of that a series of small- and moderate-sized earthquakes occurred in a relatively short time slice and confined to a definite area. They have magnitudes close to each other.

2. Stratigraphic Outline of Study Area

The rocks exposed in the study area can be subdivided into four categories based on their lithology, age, and contact relationships. These are, from oldest to youngest, the low-grade Karadağ metamorphic rocks, the Kestanbol granitoid pluton, the Ayvacık-Balabanlı volcanic rocks, the fluvial to shallow marine sedimentary sequence (Gülpınar Group), and the Quarternary basin fill or neotectonic fill (Figure 2). Both the Cambrian-Upper Permian Karadağ metamorphic rocks and the Upper Oligocene-Lower Miocene Kestanbol granitoid pluton are older basement rocks. The latter intrudes the metamorphic rocks but displays a gradational transition into the

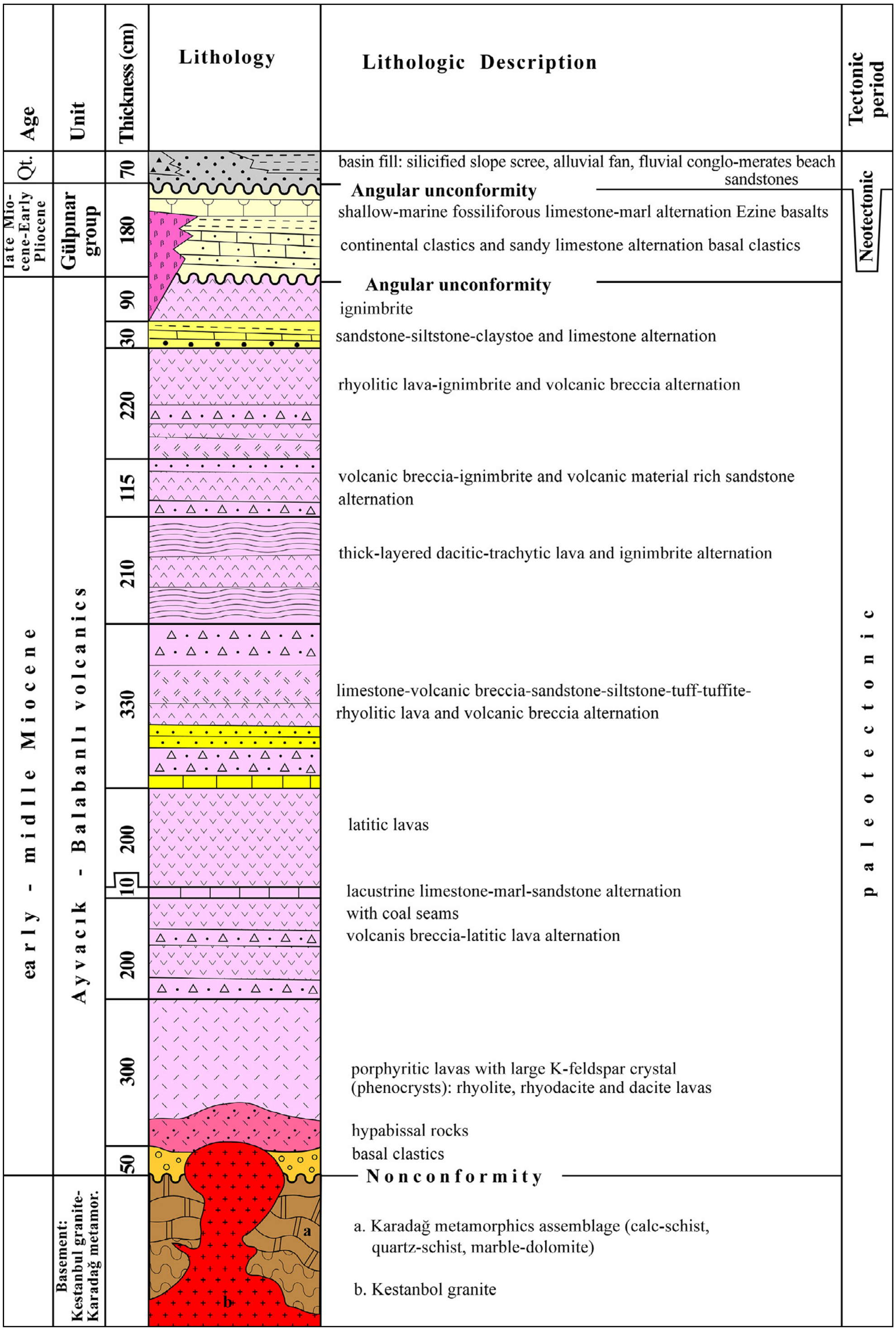

Figure 2- Combined stratigraphic column of the study area.

finegrained hypabyssal rocks with a composition same as those of the pluton (Şahin et al., 2010). At the top, these intrusive rocks are overlain conformably by the volcanic rocks. The Kestanbol pluton is also drilled at a shallow depth inside the Tuzla Dome, which is the key structure for the Tuzla geothermal field controlled by the active faults (Şamilgil, 1983; Gevrek et al., 1985).

Based on the prominent product in the sequence, volcanic rocks are subdivided into two categories (Karacık and Yılmaz, 1998). These are the lava-dominated Ayvacık volcanic rocks and the ignimbrite-dominated Balabanlı volcanic rocks. They are cropped out on the northern footwall and southern hanging wall blocks of the Çamköy master fault segment respectively (Figure 3a). The Ayvacık volcanic rocks comprise relatively lower section of the volcanic sequence. They consist of gray and black rhyolite, rhyodacite and dacite lavas. They rest directly on the underlying hypabyssal rocks at the bottom and then are followed upward by the alternation of latitic lava, volcanic breccia, lacustrine limestone, marl and sandstone. The Balabanlı volcanic rocks are composed mostly of pyroclastites, among which ignimbrites are prominent. Ignimbrites are represented by three sections. These are, from bottom to top, base-surge deposits, welded ignimbrite and non-welded tuff. Ignimbrite packages range from several meters up to 80 m in thickness. Common lavas comprising the Balabanlı volcanic rocks are latitic and andesitic lavas. The K/Ar ages obtained from various levels of the Ayvacık-Balabanlı volcanic sequence range from 21.5 Ma to 15.9 ± 0.4 Ma, i.e., they are early Middle Miocene in age (Borsi et al., 1972; Ercan et al., 1995). The third unit in the study area is the Gülpınar Group. It is exposed widely along the coastal area between Akliman Bay in the southwest and the Babadere settlement in the northeast (Figure 3a). In addition, it also occurs in diverse sized and discontinuous outcrops around Kızılkeçili, Yukarıköy and Tabaklar villages. The Gülpınar Group rocks rest on all of abovementioned rocks with a regional angular unconformity. They begin with fluvial clastic rocks on the erosional surface of older rocks and then continue upward with the sandstone, siltstone, sandy limestone, and shale-marl alternation. This alternation is succeeded by medium to thick-bedded and fossiliferous shallow marine limestone at the top (Figure 2). The limestone and marls are full of micro- and macro-fossils such as Ostracod, Ostrea, Brachiopod and Gastrapod. Basal clastics of this sedimentary sequence are unsorted and polygenetic in composition. They contain pebbles derived from metamorphic rocks, granitoid pluton and the volcanic rocks. Pebbles are set in a volcanic material rich sandy matrix and range from sand size to 30 cm in diameter. In the east and outside the study area (in the Ezine-Bayramiç basin) the fluvial conglomerates alternate with the alkali olivine basaltic lavas (the Ezine Basalt). Same basalts crop out and cut across the Balabanlı volcanic rocks around the Kuşkaya promontory along the northern coastal area of the Edremit Gulf (Figure 3a). The K/Ar method applied on samples of the Ezine basalt yielded a radiometric age of 11.0 ± 0.4 Ma-8.4 ± 0.3 Ma (Ercan et al., 1995), i.e., alkali olivine basalts are late Miocene in age and the product of a younger magmatic activity. Consequently the Gülpınar Group is also late Miocene-early Pliocene in age. The last and youngest sedimentary sequence in the study area is the modern basin fill. It exposes widely in the Ayvacık, Behramkale, and Tuzla strike-slip basins (Figure 3a). It consists of coarse grained marginal and fine grained axial plain facies. These are the slope scree, fault terraces, alluvial fan, flood plains, beaches and delta deposits. In general, they are unsorted, weakly lithified to loose and polygenetic in composition. Modern basin fill is non-deformed (flat-lying), and overlies all of the pre-Quaternary rocks with a regional angular unconformity which reveals that the major inversion in extensional palaeotectonic regime occurred at the beginning of Quaternary. The deposition of modern basin fill is still lasting under the control of an active strike-slip faulting.

3. Tectonic Settings

3.1. Faults and Faulting Mechanism

In the identification of faults, both the seismological and the geological criteria (morphotectonic and fault plane related criteria) were used. These are the steep scarps, sudden break in slope and back-tilting of fault-bounded blocks, triangular facets, deflected to offset drainage systems, the incised stream valleys carved deeply into their beds, fault parallel aligned cold to hot water springs, sag ponds, pressure ridges, fault parallel aligned to degraded alluvial fans and deltas, contractional to extensional double bending and stepovers, braided pattern of faults peculiar to strike-slip faulting, tectonic juxtaposition of older rocks with the Quaternary alluvial sediments, faulted uplifted dissected and fault suspended terrace deposits, liner to actively growing basins, curvilinear fault traces, long, deep and narrow depressions (fault corridors), hanging valleys, active earth flows, sudden change in strike and dip amounts of rocks, strips of intensely crushed to pulverized rocks, ruins of ancient settlements, well-preserved slickenside, the earthquakes and their focal plane solution diagrams and the epicenters distribution pattern. These are common and widespread criteria for the recognition and identification of faults. These criteria will not be repeated once more for each of the

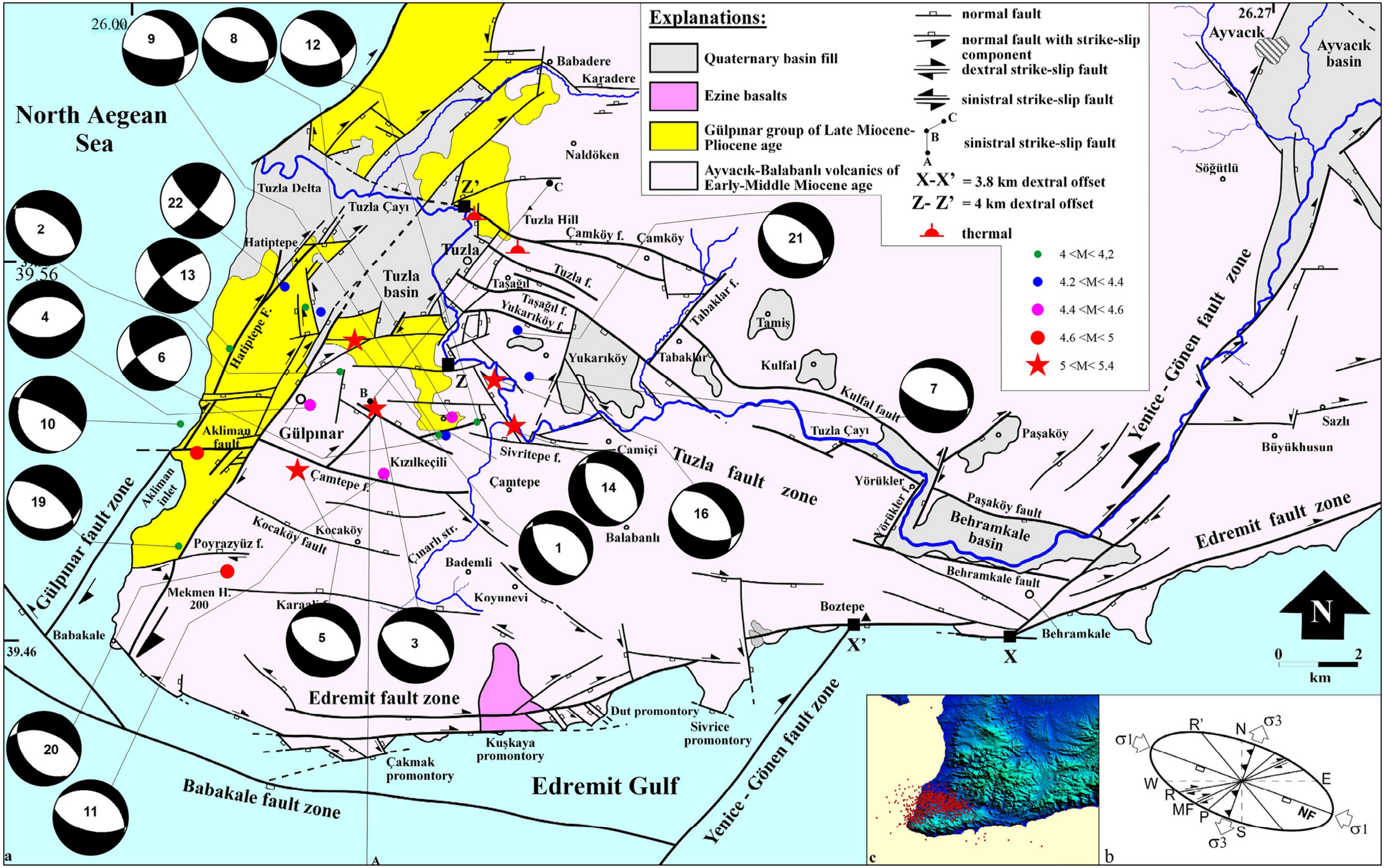

Figure 3- Seismotectonic map of the Gülpınar-Tuzla (Ayvacık-Çanakkale) earthquake area and near environment (the seismologic data from AFAD, 2017 and GFZ, 2017; the offshore faults were drawn by using Güney et al., 2001, Yaltırak et al., 2013 and the bathymetric maps of general command of the map; the onshore geological map is original and it was carried out directly in the field).

faults below. However, the origin, faulting mechanism and earthquake-induced faults are described and analyzed below.

Both the normal and strike-slip faults were reactivated and caused the occurrence of a moderate- and small-sized earthquakes cluster in the Gülpınar-Tuzla area (Figure 3b). Focal mechanism solution diagrams of the earthquakes of $4.0 \leq Mw \leq 5.3$ indicated that the major principal compressive stress (σ1) is operating in approximately WNW direction. However at a regional scale, i.e., in the central to northern Aegean Sea and Biga Peninsula, this direction is changing spatially from WNW to WSW, and it may be accepted that the average operation direction of σ1 is E-W. This stress system is responsible for the development of the strike-slip faulting pattern characterizing the study area (Figure 4).

In addition, angular relationships among components of strike-slip faulting pattern may change in time as a natural response to both internal and external rotations (Figure 3c). Based on the operation direction of the σ1, the WNW-trending fault segments are oblique-slip normal faults, while the NW-, NE- to ENE-trending fault segments are sinistral strike-slip and dextral strike-slip faults respectively (Figures 3a, c and 4). It is also known that normal components of fault segments increase as their strikes approach to the orientation of σ1. The strike-slip faulting pattern comprising the structural configuration of the study area is represented by the NE-trending Gülpınar, the NE-trending Yenice-Gönen, the E-W-trending Edremit and the WNW-trending Tuzla fault zones (Figure 3a). Earlier three fault zones are strike-slip, while the latter is normal fault in character. However the prominent fault segments comprising the Edremit fault zone have a considerable amount of normal components. Indeed, the most of fault segments comprising the EFZ were originally normal faults inherited from the Miocene-Pliocene extensional palaeotectonic period. They have taken a significant role in the evolution of Edremit palaeotectonic graben. This is evidenced by the well-preserved slickenside with two sets of slip lines of dissimilar origin overprinted on each other on the pre-Quaternary sedimentary sequence and volcanic rocks. The EFZ was reactivated to be a secondary dextral strike-slip fault (R-shear in Figure 4) with a

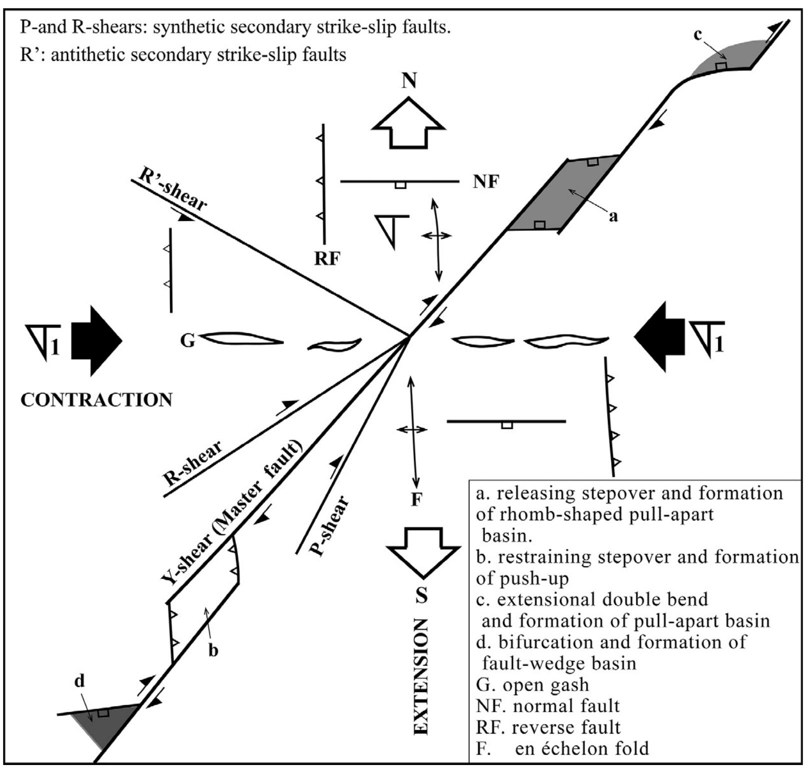

Figure 4- Faulting mechanism in the central to northern Aegean strike-slip neotectonic domain including the study area.

considerable amount of normal component during the Quaternary strike-slip neotectonic period. In general, faulting mechanisms are classified into three categories based on the orientations of three stress axes (least σ3, intermediate σ2 and greatest principal axes σ1). These are the thrust-reverse, strike-slip and normal faulting mechanisms in which σ3, σ2 and σ1 are vertical to subvertical in position respectively. Only mechanism is the strike-slip faulting by which both contractional and extensional features may develop simultaneously, i.e., folds, thrust to reverse faults, strike-slip faults and normal faults may develop under the control of strike-slip faulting mechanism (Figure 4). Therefore, this mechanism is also accepted as a model to explain the opening and closure histories of basins. In addition, in this mechanism both the amount and duration of motion on each fault/fault zone are not constant and continuous, i.e., they decrease, increase or stop from time to time. For this reason, different faults or fault zones originated or reactivated from the same strike-slip faulting mechanism may cut and offset to each other in time as in the case of the Gülpınar-Tuzla earthquake area (Figure 3a). These fault zones and the origins of the abovementioned earthquakes are described below.

3.2. Tuzla Fault Zone (TFZ)

This structure was previously defined and named as a single fault, the Tuzla Fault, by Karacık and Yılmaz (1998). Indeed it is a zone of deformation consisting of numerous structural fault segments (Figure 3a). It is about 2.8-11 km wide, 19 km long and WNW (N65°W)-trending normal fault zone with considerable amount of sinistral strike-slip component. It is represented by the open fractures (NR) parallel to the σ1 in Figure 3c). The TFZ is confined into a westward widening wedge-shaped area bounded by the YGFZ in the east, the EFZ in the south and the GFZ in the west (Figure 3a). It consists of 0.4-11 km long, E-W- to WNW-trending, both southerly and northerly dipping (up to 60°) normal fault segments (Figures 3a and 5). The Ayvacık-Balabanlı volcanics are crossed, sheared and brecciated by these fault segments (Figure 6). They display a graben like depression truncated and downthrown by the GFZ in the west (Figure 7). In addition, both the NE-trending dextral and NW-trending sinistral strike-slip fault segments also occur within the TFZ. Some of them are the Tabaklar, Yörükler and the Sivritepe dextral strike-slip faults. The first two segments cut and offset the northernmost normal fault in the dextral direction and divide it into three segments, namely the Çamköy, Kulfal and Paşaköy faults (Figure 3a). The Tuzla River (Çay) is the major drainage system in the Gülpınar-Tuzla earthquake area. In general, it flows in WNW direction and follows the traces of both the normal and strike-slip fault segments. For this reason its flow direction varies frequently and displays an uneven bed in shape throughout the TFZ. However it changes the flow direction toward NNE and gains a relatively straight bed when it enters into the NNE-trending GFZ (Figures 3a and 7).

The northerly-located but southerly-dipping fault segments comprising the TFZ are more active than others. It was proved once more by the epicenters distribution pattern of the 2017 Gülpınar-Tuzla earthquake cluster (Figure 3b). These are, from NW to SE, the 11 km long Çamköy, 3.3 km long Tuzla, 7.7 km long Taşağıl, 3 km long Yukarıköy, 7.8 km long Kulfal and the 5.5 km long Paşaköy faults (Figure 3a). Based on their lengths, magnitudes of peak earthquakes to be sourced from these faults are the Mw = 6.2, 5.6, 6.1, 5.6, 6.1 and 5.8 respectively (Wells and Coppersmith, 1994). It seems that the independent earthquakes No. 1, 3, 5, 14 and 16 might have been originated from

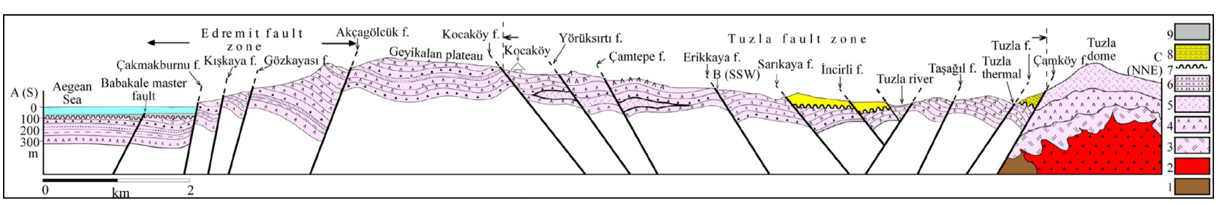

Figure 5- Geological cross-section along the line A-B-C in Figure 3. It illustrates fault-controlled Tuzla geothermal area, internal structure of the Tuzla dome and both the Tuzla and Edremit fault zones. 1. Karadağ metamorphic rocks, 2. Kestanbol granitoid pluton, 3. Hyp-abyssal intrusive rocks, 4. porphyritic lavas, 5. ignimbrites, 6. various lavas and pyroclastic alternation with sedimentary intercalations, 7. angular unconformity, 8. terrestrial and shallow sea water sedimentary sequence (Gülpınar Group), and 9. modern basin fill.

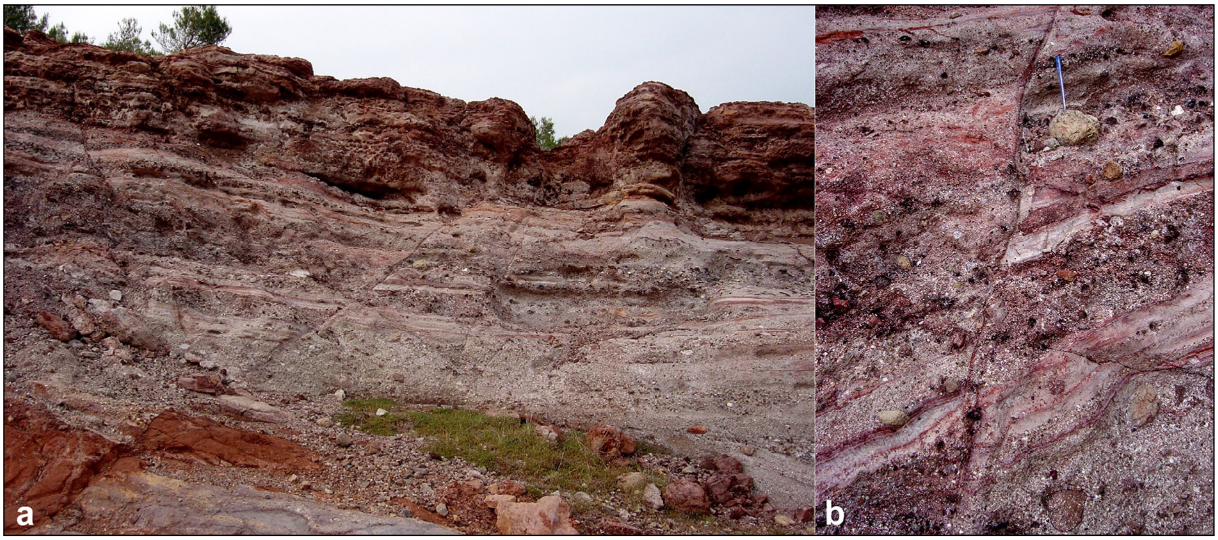

Figure 6- a) and b) field photographs illustrating normal faults developed in Lower-Middle Miocene tuff-volcanic breccia alternation cut and deformed (crushed, brecciated and sheared) by the Tuzla fault zone.

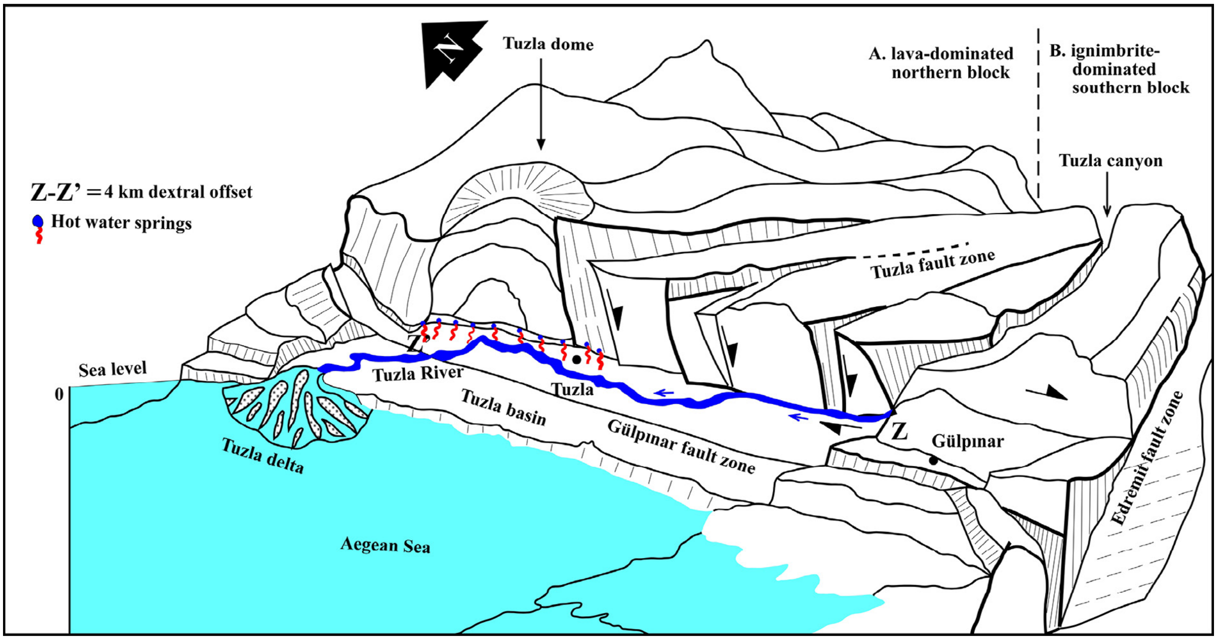

Figure 7- Sketched block diagram depicting the graben-like structure of the Tuzla fault zone truncated and offset in right-lateral direction (Y-Y' = 4 km) by the Gülpınar fault zone.

the first four fault segments based on the earthquakes parameters such as the dip amount to dip direction, focus depth, epicenter site and the patterns of the focal mechanism diagrams (Figure 3a). The latter parameter also indicates that the extension direction in the study area is NNE (Figure 3a). This is also evidenced by the palaeostress analysis of slipplane data measured on slickensides of the fault segments (Figures 8a, b and c). Several reverse faults, which dip steeply to NNE, were also observed on the southern slope of the Tuzla dome. But they could not be mapped due to the small scale of the map. Indeed these faults might have been originated from vertical motion related to the forceful injection and emplacement of the Kestanbol granitoid pluton. The Upper Miocene-Pliocene Gülpınar group overlies with an angular unconformity the Oligo-Miocene Kestanbol pluton. Its basal clastics contain pebbles of pluton. This observation reveals that the emplacement and uplift of the pluton were completed and began to be eroded before late Miocene. Consequently, outcrop scale reverse faults might have formed in palaeotectonic period not during the Quaternary neotectonic period.

3.3. Gülpınar Fault Zone (GFZ)

This structure was previously defined and introduced to the literature as a single fault, the Gülpınar fault (Karacık and Yılmaz, 1998). Indeed it is an approximately 1.7-5.5 km wide, 37 km long and N 20°-35° E-trending dextral strike-slip fault zone with a considerable amount of thrust component, by which its southeastern block was uplifted up to 0.4 km with respect to the western block. The Gülpınar fault zone is located in the area between Dalyan Town in the northeast and 1.5 km west of Babakale in the southwest along the coastal area of Aegean Sea (Figure 1b). The 19 km long southwestern section of fault zone is included in the study area (Figure 3a). However its 18 km long northeastern section lies outside. The external section was previously mapped and named as a single fault (the Kestanbol Fault) and then interpreted to be an oblique-slip normal fault (Emre and Doğan, 2010). The Gülpınar fault zone consists of numerous closely to medium spaced (0.1-2 km) and diversesized (0.2-9.5 km) fault segments of dissimilar trends such as NE, NW and E-W. The prominent and longer segments are NE in trend (Figure 3a). In and outside the study area, the Paleozoic metamorphic rocks, the Upper Cretaceous ultrabasic rocks, the Oligo-Miocine Kestanbol pluton, the Lower-Middle Miocene felsic volcanic rocks (Ayvalık-Balabanlı volcanics), the Upper Miocene-Middle Pliocene sedimentary sequence (Gülpınar group) and the Quaternary modern basin fill are cut, displaced in both vertical (0.4 km) and lateral (4 km) directions and juxtaposed tectonically with to each other in places by fault segments. The Tuzla River is offset (up to 4 km) in the dextral direction by several fault segments when it enters into the Tuzla strike-slip basin developed along the Gülpınar fault zone (Z-Z’ = 4 km in Figures 3a and 7). In the same way, the Gülpınar fault zone is also cut and displaced up to 2 km in both sinistral and dextral directions by the NNW- and NW-trending faults. One of these offset structures is exposed well around Kösedere village outside and 0.5 km north of the study area, i.e., there is a strong interaction among the fault segments of dissimilar origin and trends comprising the strike-slip fault pattern. This is evidenced strongly by thermal waters, which use their intersection areas, such as the Kestanbol and Tuzla thermals, and come out of the ground (Figure 3a).

The 4.4 km long and NE-trending Hatiptepe fault segment of the Gülpınar fault zone reactivated on Monday 24 March 2017 and caused to the occurrence of a small sized (Mw = 4.2), shallow-focus (h = 9.7 km) and independent earthquake of pure strike-slip origin (No.22 in Figure 3a). Based on the length of the longest (9.5 km) segment, the magnitude of the peak earthquake to be sourced from the Gülpınar fault zone is Mw = 6.2 (Wells and Coppersmith, 1994). This seismic data reveals that the Gülpınar fault zone is a dextral strike-slip fault not oblique-slip normal fault as has been reported in previous works (Karacık and Yılmaz, 1998; Emre and Doğan, 2010). This fault zone is represented by the secondary synthetic strikeslip fault (P-shear in Figure 3c).

3.4. Yenice-Gönen Fault Zone (YGFZ)

This is the most significant and active dextral stike-slip fault zone (Şaroğlu et al., 1987; Barka and Kadinsky-Cade, 1988; Herece, 1990; Kürçer et al., 2008). It includes the master fault (Y-shear or MS in Figure 3c) of the southern strand of the NAFS. In general, the YGFZ trends NE and has a total length of 335 km. It consists of two sections, the onshore and the offshore sections respectively. The 165 km long onshore section is located in the area between Gönen County in the northeast and Behramkale in the southwest (Figures 1b and 3a). It was previously studied and documented well (Herece, 1990; Kürçer et al., 2008; Koçyiğit, 2011; Yaltırak et al., 2013). The 6-20 km wide and N55°-60°E-trending onshore section consists of numerous parallel and subparallel, closely to widely spaced (0.4-8 km) and diverse-sized (0.5-40 km) structural fault segments. A limited number of N-S-, E-W- and NW-trending fault segments in the nature of reverse, normal and sinistral stike-slip faults, respectively, also occur in this zone. The onshore section of the YGFZ runs in southwest direction across the Gönen River, Koca Çay valley, Yenice County, Zeybekçayırı and the northern foot of the Kazdağ mega pressure ridge in the east (Figures 9 and 10). Approximately 3 km east of Ayvacık County, it enters into the study area, bends south at about 30° and then runs for about 16 km in SW direction up to Behramkale Town (Historical Asos City) along the

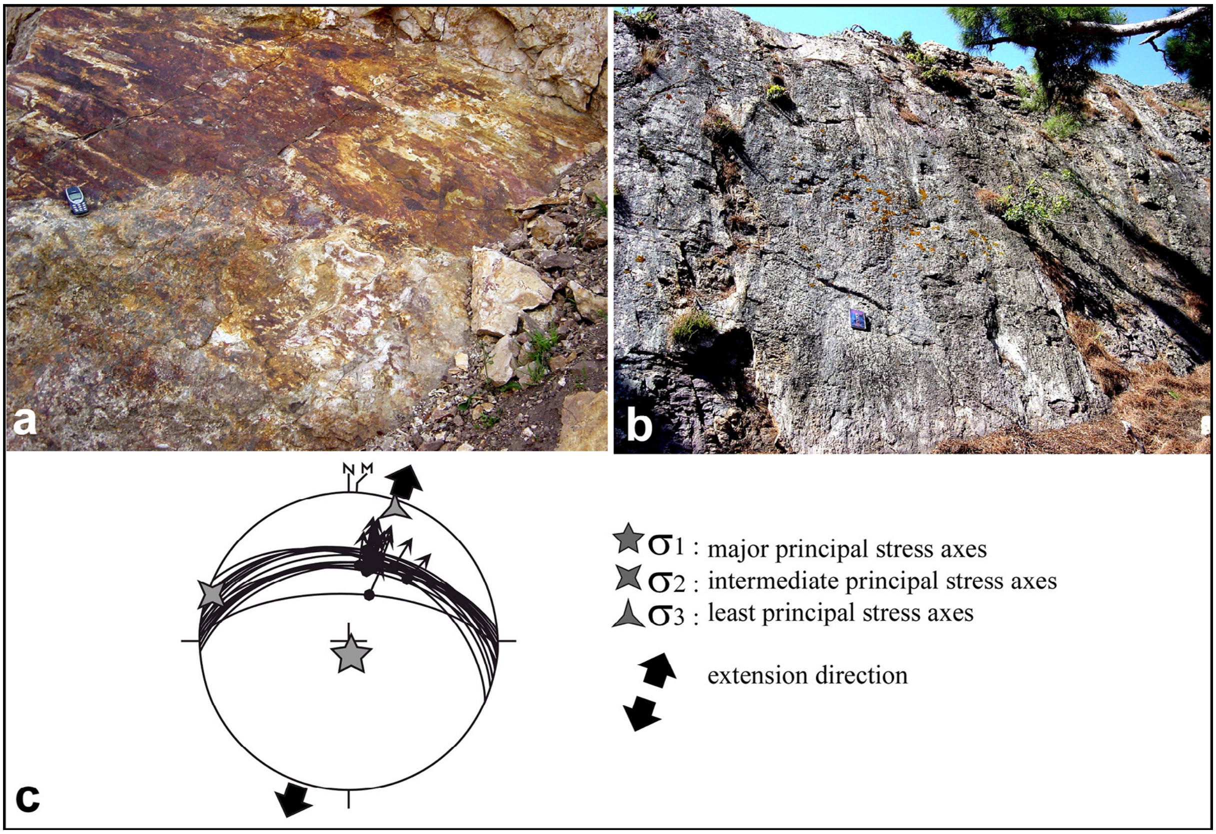

Figure 8- a) and b) field photographs of normal fault slickensides, and c) the stereographic plot of slip-plane data on the Schmidt lower hemisphere net.

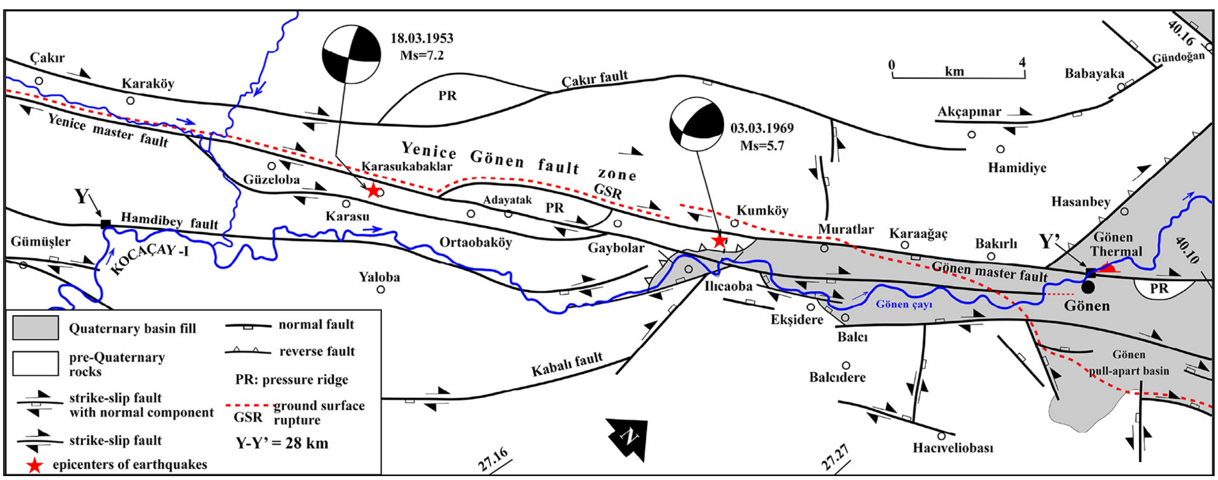

Figure 9- Seismotectonic map of the Gönen section of the Yenice-Gönen Fault zone (YGFZ).

Tuzla Çayı Canyon. At this locality, it is cut and offset in the right lateral direction by the Edremit fault zone along the northern margin of Edremit Gulf (X-X'= 3.8 km in Figure 3a). At the point X' near Boztepe, it enters into sea water and then continues in the same direction to be the offshore section (southern margin boundary faults of both the Babakale and Skyros basins) along the sea bottom of Edremit Gulf. Along the whole length of the onshore section, various rocks of dissimilar age and facies are cut and divided into numerous lenticular bodies by the bifurcation, rejoining and rebifurcation of fault segments comprising the fault zone. Thus a braided strike-slip fault pattern, which is peculiar to the strike-slip faulting, develops (Figures 9 and 10).

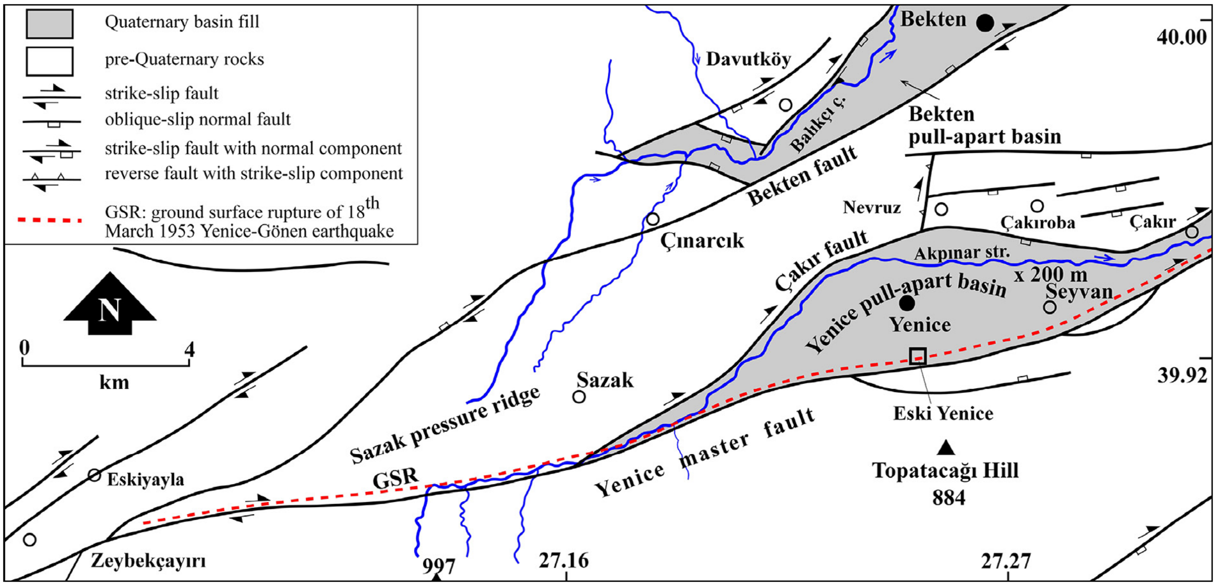

Figure 10- Fault map illustrating the Yenice-Bekten pull-apart basins and ground surface rupture of the 8 March 1953 Yenice-Gönen earthquake.

In this pattern long axes of lenticular bodies are nearly parallel to the general trend of the fault zone. In addition, numerous pressure ridges and pull-apart basins have developed due to the uplift and subsidence of these fault bounded lenticular bodies. The most outstanding of them are, from northeast to southwest, the Gönen, Yenice, Bekten and Ayvacık basins and the intervening Kazdağ mega pressure ridge. Some major drainage systems, such as Gönen Çayı, Koca Çay and the Tuzla Çay, are fault-controlled and offset. For instance, the Koca Çay-Gönen Çay drainage system is offset up to 28 km in the right lateral direction by the onshore section of the YGFZ (Y-Y' in Figure 9). This value implies a uniform slip rate of 10.9 mm/yr (Koçyiğit, 2011). Whereas it has been previously reported that the total right-lateral displacement accumulated along the Yenice section of the fault zone is only 2.8 km (Herece, 1990). Based on the length of the longest (40 km) fault segment comprising the onshore section, the magnitude of the peak earthquake to be sourced from it is Mw = 7.0 (Wells and Coppersmith, 1994). Its truthfulness was proved by the reactivation of the Yenice-Gönen section and occurrence of the 18 March 1953 Yenice earthquake of Ms = 7.4 (Tan et al., 2008). This destructive earthquake has also led to the development of an approximately 40 km long surface rupture with a maximum 1.3 m vertical and 4.2 m right-lateral displacements in the area between Kalfaköy (Gönen) in the northeast and south-southwest of Eskiyayla settlement (Yenice) in the southwest (Figures 9 and 10) (Herece, 1990; Kürçer et al., 2008). This destructive earthquake attracted attentions of several researchers, who have carried out detailed but local field geological mapping and palaeoseismological studies (Pınar and Lahn, 1952; Ketin and Roesly, 1953; Herece, 1985, 1990; Kürçer, 2006, 2008). Based on the palaeoseismological data, a recurrence interval of 660 ± 160 years was suggested for the large destructive earthquakes to be sourced from the Yenice-Gönen master fault (Kürçer et al., 2008, 2019). These authors have also reported that the Yenice-Gönen master fault has been active since Miocene and the slip rate along it is about 6.3 mm/yr. If this is true, the total right lateral displacement accumulated along the Yenice-Gönen fault since Miocene must be at least 32 km. Whereas they have reported that it was only 2.8 km, i.e., there is a contradiction between the reported slip rate (6.3 mm/yr) and the total right-lateral displacement (2.8 km). Consequently, the total right-lateral displacement on the Yenice-Gönen fault zone is much more than 2.8 km. It was determined to be 28 km (Y-Y' = 28 km in Figure 9) in the present study.

The 175 km long offshore section runs across the Aegean Sea floor between Boztepe along the northern margin of Edremit Gulf in the northeast and the Skyros Island in the southern North Aegean Sea in the southwest (Figures 1b and 3a). It is about 60 wide, 180 km long and N50°-60°E trending zone of deformation. The offshore section consists of NE-trending dextral strike-slip faults and the intervening NW-trending oblique-slip normal faults. Three large pull-apart basins developed within the offshore southern strand. These are the Bozcaada, Babakale and the Skyros basins (Figure 1b). The deep, long and narrow depressions bounded by steep fault scarps, closely spaced and straight bathymetric contours, positive and negative flower structures, active underwater earthflows and intensely deformed Quaternary sediments are common morphotectonic criteria for the existence of active faults (Eryılmaz and Yücesoy, 1999; Güney et al., 2001; Koukouvelas and Aydın, 2002; Kurtuluş et al., 2009; Yaltırak et al., 2013; Gürer et al., 2016). On the other hand, this area is also seismically very active as indicated by both the historical and recent destructive earthquakes, such as the 14 February 1672 Babakale-Lesvos Island and the 4 March 1967, 19 February 1968, 19 December 1981 and the 27 December 1981 Skyros Island earthquakes, occurred within it (No. 7, 8, 11 and 12 on Table 1 and Figure 1b) (Papazachos et al., 1984, 1991; Ambraseys and Finkel, 1995). Both the onshore and the offshore sections of the major southern strand are linked to each other by the Bozcaada, Babakale and Edremit Gulf strike-slip basins and related NNW-trending oblique-slip normal faults. In this frame, the NE-trending southern and the northern margin boundary faults of both the Skyros and Babakale basins are the offshore extents of both the YGFZ and the Bayramiç-Ezine fault zone respectively. Consequently the southern strand of the NAFS continues across the Biga Peninsula and the North Aegean Sea floor up to Skyros Island in the farther southwest (Figure 1b).

3.5. Balıkesir-İzmir Fault Zone (BİFZ)

This is an about 5-25 km wide, 250 km long and NE-trending dextral strike-slip fault zone located in the area between Lake Ulubat in the northeast and Samos Island in the southwest (Figures 1a and 1b) (Uzel and Sözbilir, 2008; Koçyiğit, 2012, 2020). Indeed, the BİFZ is an originally palaeotectonic structure inherited from the late Cretaceous. It reactivated to be a megashear zone in the nature of dextral strike-slip fault zone in the Quaternary neotectonic period. It forms a transitional zone between the easterly located southwest Anatolian extensional and westerly located central to northern Aegean compressional provinces (Koçyiğit, 2012). These two neotectonic regimes interact with each other along this transitional zone. The BİFZ is seismically very active. This was proved once more by the occurrence of several earthquake clusters such as the 10 December 2019 Balıkesir, 22 January 2020 Akhisar and 18 February 2020 Kırkağaç earthquakes (EMSC, 2019, 2020). The seismic activity migrated along the BİFZ in a southwestward direction up to Saruhanlı County, and it is still lasting. One of the type localities, where faulting-induced morphotectonic features are exposed well, of the BİFZ is the Kepsut County. It is located along the eastern margin of the Balıkesir pull-apart basin. In this area, the Susurluk River is displaced up to 23 km in the dextral direction by the BİFZ (P-P’= 23 km in Figure 11). This value implies a uniform slip rate of 8.9 mm/yr along this fault zone.

3.6. Edremit Fault Zone (EFZ)

This is an approximately 2-12 km wide, 160 km long and ENE-trending dextral strike-slip fault zone with a considerable amount of normal component. It is located between Balıkesir in the east and Babakale in the west (Figures 3a and 12). Its western half and various characteristics including kinematics and seismicity were previously studied and reported (Kurtuluş et al., 2009; Koçyiğit, 2011; Altınok et al., 2012; Gürer et al., 2016; Sözbilir et al., 2016). The EFZ determines the southern outline of Biga Peninsula. It contains four strike-slip basins. These are, from E to W, the Balıkesir, Gökçeyazı, İvrindi and Edremit Gulf basins (Figures 3a, 11 and 12). In terms of these basins, the EFZ is linked to the easterly located Balıkesir-İzmir (BIFZ) and northerly located Ilıca-Darıca dextral strike-slip fault zones (Figures 11 and 12). The Edremit Gulf basin and the Kazdağ mega pressure ridge, which rises up to 1700 m above sea level along its northern margin, have been interpreted to be a graben and horst in some of previous works (Yılmaz et al., 2000, Güney et al., 2001). As is to be explained in the sentences below, this interpretation is not true. The EFZ consists of numerous parallel to subparallel, closely to medium-spaced (0.2-4 km) and diverse-sized (1-40 km) structural fault segments. They are ENE, N-S, NW and NE in trend, but the ENE-trending segments are more prominent and longer than others (Figures 3a and 12).

Some of these fault segments are inherited from the Pre-Quaternary palaeotectonic period. They cut across various rocks (e.g., Paleozoic Kazdağ metamorphic rocks, Permo-Triassic Karakaya Complex, Upper

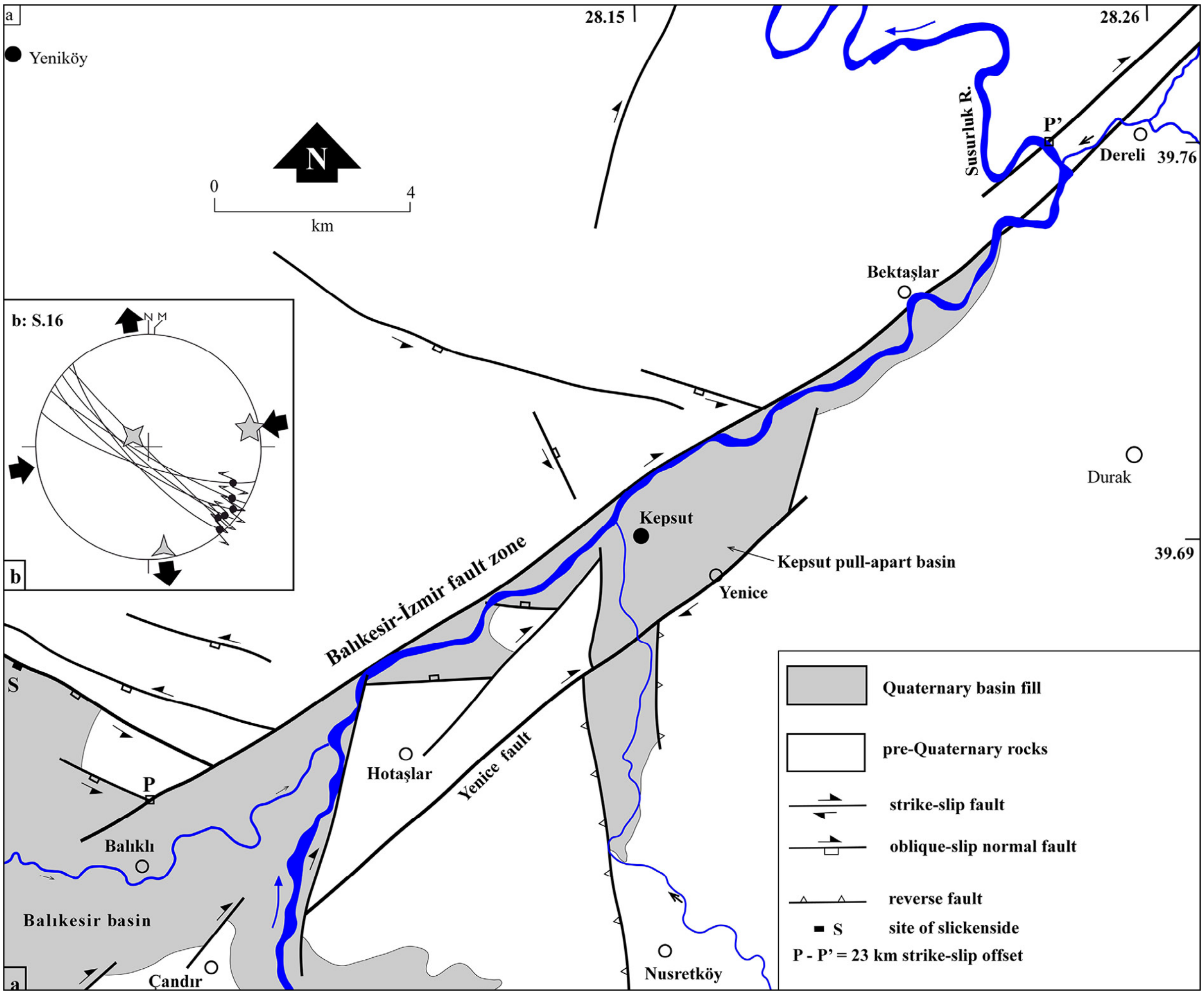

Figure 11- Neotectonic map of the Kepsut section of the Balıkesir-İzmir Fault Zone (BİFZ). It illustrates the easternmost tip of the Edremit fault zone (Balıkesir pull-apart basin) and the offset drainage system (Susurluk River) along the BİFZ.

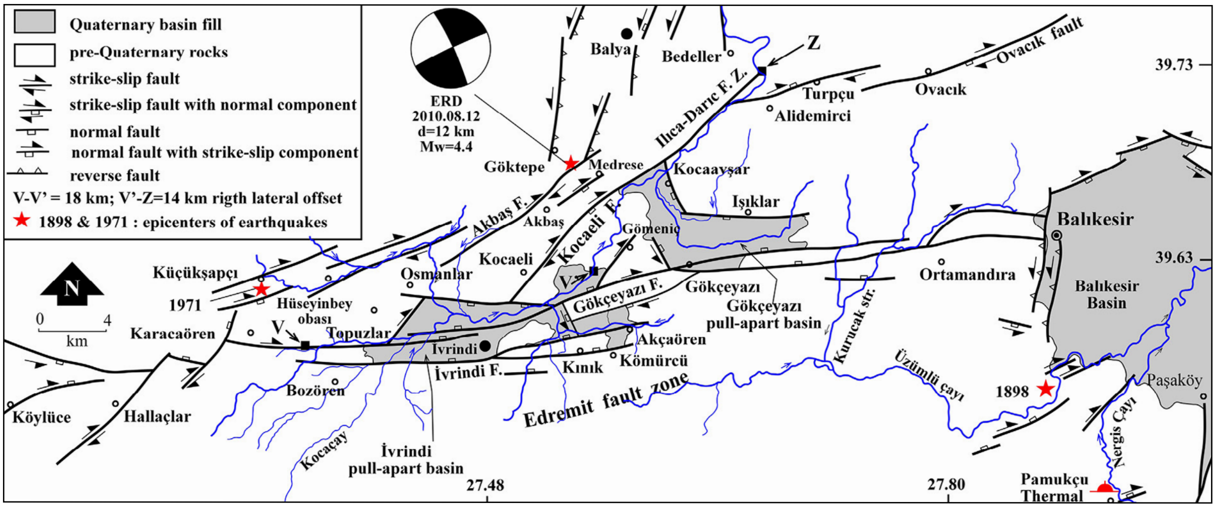

Figure 12- Seismotectonic map of the eastern half of the Edremit fault zone (EFZ).

Cretaceous-Paleocene ophiolitic mélange to ultramafic rocks, Oligocene volcanic rocks, Oligo-Miocene granodiorite, Lower-Middle Miocene volcanic rocks and the Upper Miocene-Pliocene sedimentary sequence), and tectonically juxtapose them with each other and also with the Quaternary neotectonic basin fill. The thickness of the modern basin fill of Edremit Gulf basin ranges from 200 m to 700 m (Emre and Doğan, 2010), and it rests with an angular unconformity on the Pliocene erosional surface of the underlying older deformed rocks. Thus, the total throw amount accumulated on the EFZ can be estimated as 2-2.5 km by the comparison of the 1700 m high onshore erosional surface of Pliocene age with the 300-800 m deep offshore erosional surface of the same age. In addition, some structural and geographical features are displaced in right-lateral directions. Around İvrindi in the farther east of Edremit Gulf, the Koca Çay-I drainage system is controlled and offset up to 18 km in the right lateral direction by the fault segments (V-V'=18 km in Figure 12). In the same way, based on the data obtained from the drilling studies carried out in the offshore section of the Edremit Gulf basin, it has been reported that the Lower Miocene rocks had been displaced more than 20 km in right-lateral direction (Saka, 1979; Yazman, 1996). Based on these lateral displacements, the uniform slip rates along the EFZ are 7.0-7.7 mm/yr, respectively. In addition, the multichannel seismic reflection studies carried out around Bababurnu promontory in the offshore section of the Edremit Gulf basin, some well-developed positive and negative flower structures have also been identified (Eryılmaz and Yücesoy, 1999; Güney et al., 2001; Kurtuluş et al., 2009). Consequently the great right-lateral offset, positive to negative flower structures and the WNW operation of the major principal compressive stress (σ1) altogether reveal obviously that this area has been experiencing a strike-slip tectonic regime since the beginning of Quaternary, i.e., the Edremit fault zone is represented by the synthetic strike-slip fault (R-shear in Figure 3c). In this frame, the Quaternary configuration of the Edremit Gulf is not a graben, in contrast, it is an actively growing and westward widening fault-wedge-type of strike-slip pull-apart basin. It results from the bifurcation of the EFZ into two fault zones around Hallaçlar settlement in the east of Havran County (Figures 1b and 12). These fault zones determine and control both the southern and northern margins of the basin and display basinward-facing stepped landscape bounded by the one master and a number of second order fault segments with a considerable amount of normal component. Both the mappable and outcrop scale mimics of these fault zones are well-exposed within the intensely sheared Miocene sedimentary sequence exposing along the southern fault-bounded margins of the Edremit Gulf pull-apart basin (Figure 13).

The longest (30-40 km) and most significant fault segments comprising the EFZ are the Gökçeyazı, Burhaniye and Altınoluk faults (Figures 1b and 12). Based on their lengths, magnitudes of the peak earthquakes to be sourced from these faults are Mw = 6.7 and 7.0 respectively (Wells and Coppersmith, 1994). The Altınoluk fault reactivated and led to the occurrence of the 6 October 1944 Altınoluk-Ayvacık earthquake of Ms = 6.8 and 35- 40 km long surface rupture between Akçay Town in the east and Ahmetçe village in the west along the coastal area (Ambraseys and Jackson, 1998; Emre and Doğan, 2010; Altınok et al., 2012; Yaltırak, 2003; Yaltırak et al., 2013).

4.6. February- 24 March 2017 Earthquake Cluster

4.1. Recent Seismicity

A moderate-sized (Mw = 5.3) and shallow-focus (h = 8.8 km) earthquake struck on Monday 6 February 2017 at 03: 51: 40 (local time) at the locality 2 km NNE of Gülpınar Town (AFAD, 2017). This seismic event is here named as the Gülpınar (Ayvacık-Çanakkale) earthquake due to its proximity to the epicenter (No.1 in Figure 3a). It was felt strongly over a very wide region including the cities of Çanakkale, Balıkesir and İzmir. However the severe damage was confined to Yukarıköy settlement. The Gülpınar main shock was followed by 33 aftershocks with Mw ranging from 1.4 to 4.0 in a time slice of four hours (AFAD, 2017). Approximately 7 hours later than the first event, a second independent moderate-sized (Mw = 5.3) and shallow-focus (h = 9.8 km) earthquake struck on the same day at 10:58:40 (local time) in the 1.7 km west of Kızılkeçili village (No.2 in Figure 3a). This new event is termed to be the Kızılkeçili earthquake. These two events were also followed by the occurrences of three moderate-sized, shallow-focus and independent earthquakes in the intervals of one day, three days and two days respectively in the same region. These are, in turn, the Mw = 5.2 Kocaköy, Mw = 5.0 Çamtepe and Mw = 5.3 Yukarıköy earthquakes (No. 5, 14 and

Figure 13- Field photograph of the Lower Miocene sedimentary sequence cut and deformed by the Burhaniye sub-fault zone at location~3 km SSW of Burhaniye along road cut (view to west).

16 in Figure 3a). The number of aftershocks with the Mw between 4.0 and 4.6 is 16 (Table 2). The most of seismic events described here was caused by normal faulting. On Friday 24 March 2017 at 15:19:06 (local time), a small-sized (Mw = 4.2), shallow-focus (h = 9.6 km) and independent earthquake occurred around the Hatiptepe and approximately 4 km west of Tuzla village along the coastal area (No. 22 in Figure 3a). Origin of this new event (the Hatiptepe earthquake) is strike-slip faulting, i.e., it is different than previous seismic events. These six independent earthquakes were succeeded by totally 2768 aftershocks with moment magnitudes ranging from 1.0 to 4.6 until the date of 24 March 2017. Based on data given by AFAD (2017), the total number of heavily and slightly-damaged structures are 290 and 216 respectively. In addition, one Mosque and one Thermal facility were also damaged until the date of 24 March 2017.

5. Discussion: Inversion in Palaeotectonic Regime and Onset of Neotectonic Regime

5.1. Palaeotectonic History

Starting from late Paleocene onward, the convergence between Menderes-Tauride platform to the south and the Sakarya continent to the north continued and gave rise to the occurrence of some significant events. These are: a) internal imbrication of platform sequences, b) tectonic transportation of allochthon rock assemblages (particularly ophiolitic nappes, e.g., Lycian nappes) towards farther south-southeast and their emplacement first onto the marine Eocene sequence and lastly onto the Lower-Middle Miocene marine clastics, c) the overthickening of the lithosphere up to 50-55 km (Şengör et al., 1984), d) the Barrovian type of regional metamorphism (MMM: the main Menderes Massif metamorphism) (Brunn et al., 1971; Şengör and Yılmaz, 1981; Koçyiğit, 1983; Özgül, 1984; Okay, 1986; Bozkurt, 1996, 2004; Bozkurt and Park, 1999; Sözbilir, 2005), e) a very rapid regional uplift and deposition of 2 km thick boulder block conglomerate in molassic facies (Koçyiğit, 1984), and f) exhumation of both the Kazdağ and Menderes Massifs. This long lived contractional deformation period was also accompanied by a wide-spread collisional to post-collisional magmatic activity and related felsic intrusions such as batholith, stock and dome (Ercan et al., 1985; Harris et al., 1986; Seyitoğlu and Scott, 1991; Bozkurt and Park, 1997; Genç, 1998; Karacık and Yılmaz, 1998; Wilson and Bianchini, 1999; Emre and Sözbilir, 2005; Erkül et al., 2005*a, b*; Glondy and Hetzel, 2007). They added

Table 2- Various seismic parameters of significant earthquakes happened in the Gülpınar-Tuzla (Çanakkale) area in the time slice of 6 February-24 March-2017.

No	Date	Origin time	Epicentral coordinate		Depth (km)	Magnitude	Nodal plane 1			Nodel plane 2			References
			Latitude	Longitude			strike	dip	rake	strike	dip	rake	
1	06.02.2017	03:51:40	39.5423	26.1318	8.9	Mw 5.3	142.00	54.00	-76.00	298.00	38.00	-109.00	ERD(AFAD)
2	06.02.2017	04:17:29	39.5356	26.1278	9.0	Mw 4.0	132.00	35.00	-81.00	301.00	56.00	-96.00	AFAD
3	06.02.2017	10:58:02	39.5275	26.1373	9.8	Mw 5.3	113.00	50.00	-93.00	298.00	40.00	-86.00	AFAD
4	06.02.2017	11:45:01	39.5283	26.1196	11	Mw 4.4	263.00	40.00	-92.00	86.00	50.00	-88.00	AFAD
5	07.02.2017	02:24:03	39.514	26.1161	11.9	Mw 5.2	115.00	49.00	-93.00	300.00	41.00	-86.00	AFAD
6	07.02.2017	05:15:51	39.5216	26.1568	8.9	Mw 4.3	140.00	53.00	-17.00	241.00	76.00	-142.00	AFAD
7	07.02.2017	05:17:08	39.5345	26.1796	4.9	Mw 4.2	108.00	64.00	-98.00	305.00	27.00	-75.00	AFAD
8	07.02.2017	21:00:54	39.5256	26.1585	6.9	Mw 4.4	107.00	57.00	-109.00	319.00	38.00	-64.00	AFAD
9	07.02.2017	21:35:00	39.5218	26.1548	7	Mw 4.1	91.00	66.00	-127.00	333.00	43.00	-36.00	AFAD
10	07.02.2017	22:53:30	39.5241	26.084	11	Mw 4.1	162.00	23.00	-47.00	296.00	74.00	-106.00	AFAD
11	08.02.2017	01:38:03	39.5133	26.1398	10.4	Mw 4.5	104.00	59.00	-98.00	299.00	32.00	-77.00	AFAD
12	08.02.2017	02:16:14	39.5245	26.1653	6.2	Mw 4.1	83.00	53.00	-136.00	322.00	56.00	-47.00	AFAD
13	09.02.2017	10:13:10	39.5405	26.0975	9.8	Mw 4.0	136.00	68.00	-15.00	232.00	76.00	-157.00	AFAD
14	10.02.2017	08:55:25	39.5236	26.1755	7.8	Mw 5.0	154.00	52.00	-71.00	304.00	42.00	-113.00	AFAD
15	12.02.2017	12:14:50	39.5496	26.1183	5.4	Mw 4.0	-	-	-	-	-	-	AFAD
16	12.02.2017	13:48:16	39.5336	26.17	7	Mw 5.3	107.00	49.00	-115.00	322.00	47.00	-64.00	AFAD
17	16.02.2017	00:19:00	39.5	26.1	11	Mw 4.6	116.00	43.00	-85	291.00	47.00	-93.00	GFZ
18	23.02.2017	01:55:14	39.5486	26.1225	9.5	Mw 4.3	-	-	-	-	-	-	AFAD
19	27.02.2017	22:52:23	39.4975	26.0835	10.5	Mw 4.0	96.00	29.00	-117.00	307.00	64.00	-76.00	AFAD
20	28.02.2017	23:27:34	39.492	26.0968	10.7	Mw 4.7	138.00	41.00	-65.00	286.00	53.00	-110.00	AFAD
21	20.03.2017	07:00:18	39.5446	26.1765	4.6	Mw 4.3	114.00	39.00	-105.00	313.00	53.00	-78.00	AFAD
22	24.03.2017	15:19:06	39.5541	26.1126	9.6	Mw 4.2	41.00	75.00	167.00	135.00	77.00	15.00	AFAD

a considerable amount of thermal anomaly to the overthickening lithosphere, and so, triggered both the orogenic collapse (Dewey, 1988) and the emergence of tensional forces (Dewey, 1988; Pinet and Colletta, 1990). Consequently, the contractional period was replaced by the tensional tectonic period during latest Oligocene-early Miocene (Seyitoğlu and Scott, 1991; Koçyiğit et al., 1999; Koçyiğit, 2005). This extensional tectonic regime began to affect the whole of the west and southwestern Anatolia at a regional scale throughout the Miocene-early Pliocene time, except for the intervening shortterm compressional episodes. Thus, the west-southwestern Anatolia has been divided into numerous grabens and horsts of dissimilar trend, size and age by the normal faulting. One of them was the WNW-trending older Edremit graben of palaeotectonic origin (Figure 14a).

From the tectonic point of view, there were two domains at the earlier site of both the study area and older Edremit graben during the late Oligocene. These are the western Ezine and the eastern Kazdağ areas. They were being separated by an intervening, NNE-trending and west-northwesterly dipping thrust-reverse fault zone (a mylonitic zone) (Siyako et al., 1989; Okay et al., 1990; Yılmaz and Karacık, 2001; Beccaletto and Steiner, 2005). The Kazdağ area is composed of relatively high-grade metamorphic rocks, such as amphibolite schist, gneiss and metabasites overlain tectonically by the Permo-Triassic Karakaya Complex (1a and 2 in Figure 14a) (Okay et al., 1990; Yılmaz and Karacık, 2001). The Ezine area is made up of low-grade metamorphic rocks (Karadağ metamorphic rocks) of various schist, recrystallized limestone and dolomite overlain tectonically by the combination of a thick ultrabasic to basic oceanic crust slab and mélange (Düzgören ophiolite and the Çetmi Mélange) (1b and 3 in Figure 14a) (Okay et al., 1990). These two tectonic domains were under the influence of the erosional processes occupied partly by lakes in places during the late Oligocene (Figure 14a). Starting from latest Oligocene onwards, both areas became the site of a widespread calc-alkalic volcanic activity under the control of the N-S directed extensional stress regime, in which the major principal stress axis (σ1) is more or less vertical to subvertical in position. This is evidenced by the N-S trending line of volcanic centers, the Upper Oligocene-Lower Miocene petrified wood (forest) in Lesvos Island (Katsikatsos et al., 1982), the WNW-trending older Edremit graben and its northern margin boundary normal fault (detachment fault) (Figure 14a). This time slice is also the commencement of the early exhumation phase of the Kazdağ Massif and the intrusion of granodioritic pluton (Evciler and Kestanbol plutons) into both tectonic domains (4 in Figure 14a) (Beccaletto and Steiner, 2005; Şahin et al., 2010). The volcanic activity continued up to the end of the middle Miocene and accompanied to the sedimentation in a deep lake across the older Edremit graben. So, a thick volcano-sedimentary sequence formed. This continental sedimentary sequence began with a package of relatively fine grained sandstone-siltstone at the bottom and then continued upward with the alternation of thin-bedded to laminated siltstone, mudstone, bituminous shale, limestone, turbiditic sandstone, tuff-tuffite, volcanic breccia, ignimbrite and various felsic lavas (Ayvacık and Balabanlı Volcanics) (5 and 6 in Figure 14a). Later on, this volcanic activity and the graben formation were interrupted by an intervening short and relatively local compressional stress regime at the end of middle Miocene time. This is evidenced by both the folds (open and box to isoclinal folds) developed in the volcano-sedimentary sequence, and the variation in the geochemical composition of volcanic rocks, e.g., transition from calc-alkalic nature to the subalkalic and alkalic character of the volcanic rocks (Yılmaz and Karacık, 2001). The sedimentation was lasted in a fluvio-lacustrine depositional setting along its western margin opened to the Aegean Sea waters. A subalkalic and alkali olivine basaltic volcanic activity (Ezine olivine basalt) has also accompanied to the sedimentation during late Miocene-Pliocene time. Thus, another continental sedimentary sequence with the shallow-marine intercalations (Gülpınar group) developed (Figure 2). But, the major inversion in the study area occurred in the extensional stress regime, as well as those all over Anatolian platelet, at the beginning of Quaternary (Hempton, 1987; Koçyiğit and Beyhan, 1998; Koçyiğit et al., 2000, 2001; Koçyiğit and Özacar, 2003; Çolak et al., 2012; Koçyiğit, 2013; Koçyiğit and Canoğlu, 2017).

5.2. Neotectonic History

The geologically complicated deformation pattern of Turkey has been formed by the entire demise of the southern Tethyan seaway, the Bitlis Ocean, between Indian Ocean and Mediterranean Sea, and by the continent-continent collision of northerly moving

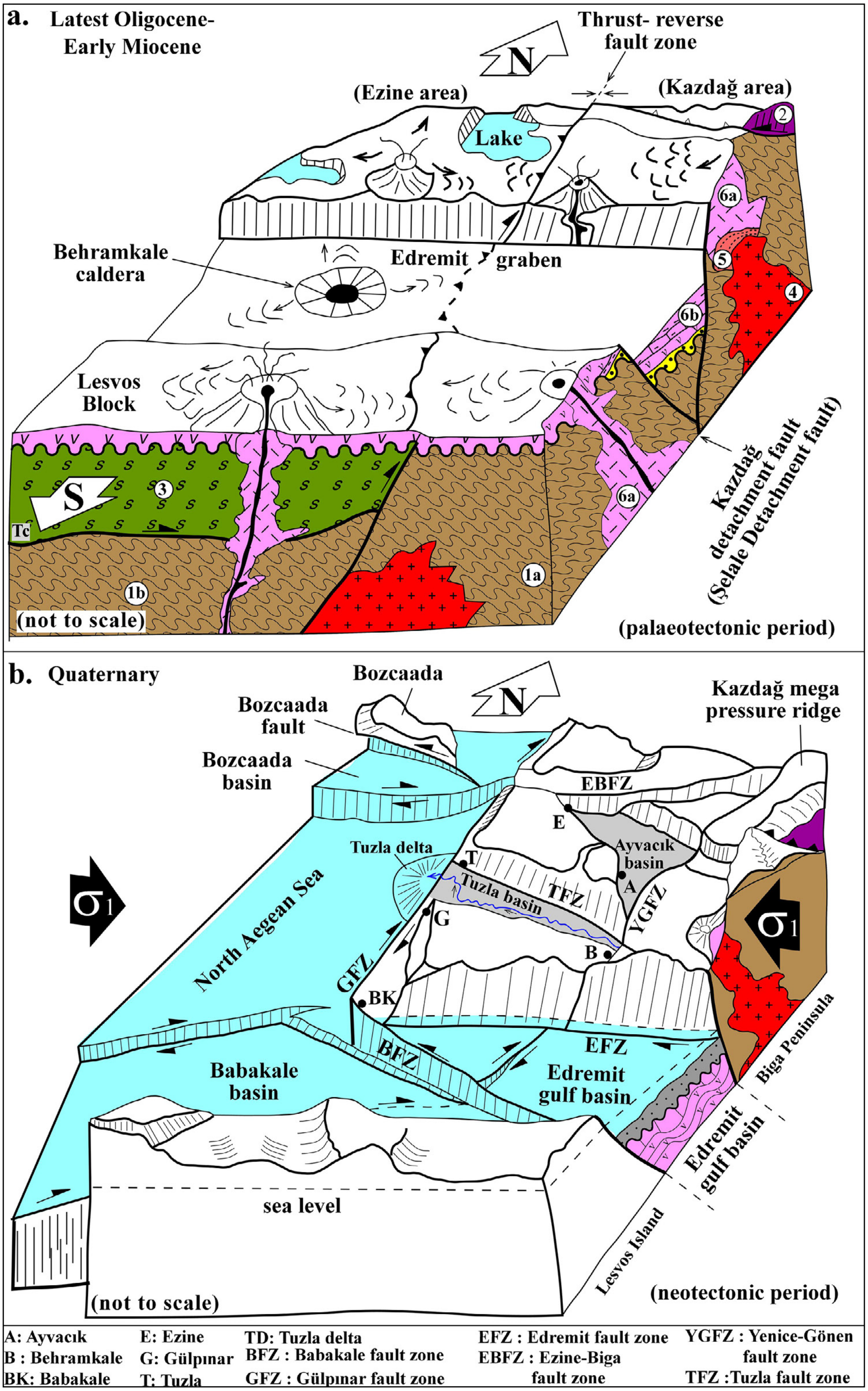

Figure 14- a) Tensional tectonic regime and graben-horst formation by the N-S directed ex-tension (white diverging arrows) (Miocene-Pliocene). 1. Karadağ and Kazdağ metamorphic rocks of Paleozoic-Triassic age, 2. Karakaya Complex of Permo-Triassic age, 3. Ophiolitic rocks of late Cretaceous age, 4-5. Granodiorite pluton and related hypabissal rocks, 6a. Calc-alkaline volcanic rocks, 6b. volcano-sedimentary sequence of terrestrial origin (older graben fill), TC. Tectonic contact, b) strike-slip neotectonic regime and development of present day configuration of the southwest tip of Biga Peninsula by the major compressive stress ope-rating in approximately WNW direction (black converging arrows) (Quaternary).

Arabian plate with the Eurasian plate in the Late Serravalian (Şengör and Yılmaz, 1981; Dewey et al., 1986). These authors accept this time slice as the onset age of the neotectonic regime in Turkey. After final collision and formation of the Bitlis suture zone, the N-S-directed intracontinental convergence between the Arabian and Eurasian plates continued over a time period of ~9 Ma. This time slice is here termed as the transitional period between the contractional palaeotectonic and the strike-slip neotectonic regimes. During this transitional period, a series of deformations such as the thickening of crust, regional tectonic uplift, formation of folds with E-W-trending axis, thrust to reverse faults, resetting of new drainage system, disappearance of marine conditions, development of short- to long-term stratigraphic gaps and prominent calc-alkaline volcanic activity occurred (Şengör and Kidd, 1979; Innocenti et al., 1980; Dewey et al., 1986; Şaroğlu and Yılmaz, 1986; Yılmaz et al., 1987; Ercan et al., 1990; Koçyiğit and Beyhan, 1998; Koçyiğit et al., 2001; Koçyiğit, 2013). The contractional deformation and development of fold-thrust belts continued until the latest Pliocene, and then this transitional period was replaced by the emergence of a new tectonic regime (prominent strike-slip faulting-related tectonic regime) (Koçyiğit et al., 2001; Aksoy et al., 2007; Çolak et al., 2012; Koçyiğit, 2013; Koçyiğit and Canoğlu, 2017). It is evidenced by the occurrence of a series of inversions such as the deformation style of faulting, types of geological structures, the nature of sedimentation and basin formation, geochemical characteristics of the volcanic activity (e.g., from calc-alkali nature to prominent alkali composition) and the nature of seismic activity. Hence the initiation age of strike-slip-dominated neotectonic regime is latest Pliocene (Koçyiğit et al., 2001). This is also proved by a regional angular unconformity separating the intensely deformed Pre-Quaternary paleotectonic rock units from the nearly flatlying Quaternary units (Koçyiğit et al., 2001).

Starting from latest Pliocene-early Quaternary onwards, the southern frontal part of the Eurasian plate was fragmented and divided into several mega and numerous micro blocks resulting in the Anatolian platelet and its margin-boundary faults, such as the dextral NAFS and the sinistral EAFS, along which the Anatolian platelet started to escape in WSW direction onto the oceanic lithosphere of the African Plate (Hempton, 1987; Koçyigit and Beyhan, 1998). In Aegean Sea, the westward motion of the Anatolian platelet was blocked and forced to move in south-southwestward by a barrier, the mainland of northern Greece. Thus, this variation in the motion direction of plate, resulted in a regional principal compressive stress (σ1) operating in approximately E-W direction (Şengör, 1980), and led to the emergence of a new neotectonic regime and province, the central to northern Aegean neotectonic province. One of the well-developed structures of this strike-slip neotectonic province is the NE-trending Balıkesir-İzmir dextral strike-slip fault zone (BİFZ) (Koçyiğit, 2020) (Figures 1a and 11). It was an originally palaeotectonic structure. In the present it forms a transitional zone between the easterly located extensional and westerly located strike-slip faulting-dominated neotectonic domains. Our study area is included in the central to northern Aegean neotectonic province. The structures and related seismic activity in the study area are the records of this new strike-slip neotectonic regime. It is being dominated by the well-developed strike-slip faulting pattern (Figures 4 and 3b), not an extensional stress regime reported by some of previous researchers (Yılmaz and Karacık, 2001; Beccaletto and Steiner, 2005; Emre and Doğan, 2010). This is the major difference between our idea and those of most of previous workers. The strike-slip faulting pattern is composed of NW- and NE-trending strike-slip faults, E–W to WNW-trending oblique-slip normal faults and an approximately NNE-trending thrust to reverse faults (Figures 3a, b and 4). This is evidenced by both the focal mechanism solution diagrams of earthquakes sourced from these faults and the palaeostress analysis of slip plane data measured on fault slickensides (Figures 3a and 8). Consequently, at a regional scale the Biga Peninsula, and at the local scale the study area gained their present day configuration under the control of the strike-slip neotectonic regime during Quaternary. This regime is still lasting under the control of the same tectonic regime and related faulting pattern (Figures 4 and 14b). It was proved once more by the occurrence of the Gülpınar-Tuzla earthquake cluster of strike-slip tectonic origin. In a short time period of 2017.02.06-2017.03.24, at least seven moderate-to small-sized independent earthquakes occurred in the Gülpınar-Tuzla (Ayvacık-Çanakkale) area. These are, in turn, the Gülpınar, Kızılkeçili, Kocaköy, Çamtepe, Yukarıköy, Derecikbağ and Hatiptepe earthquakes respectively (No.1, 3, 5, 14, 16, 13 and 22 on Table

2). The first five seismic events are the normal faulting-induced earthquakes, while the latter two are related to strike-slip faulting in origin. Based on the earthquakes parameters such as the dip amount to dip direction, focus depth, epicenter site and the patterns of the focal mechanism solution diagrams, the first five earthquakes seem to have been originated from the southerly dipping Çamköy, Tuzla, Taşağıl and Yukarıköy normal faults respectively. The latter two earthquakes were sourced from the Hatiptepe strike-slip fault, i.e., both the Tuzla normal fault zone and the Gülpınar strike-slip fault zone were reactivated by the occurrence of the Gülppınar-Tuzla earthquake cluster. The patterns of focal mechanism solution diagrams reveal a stress system, in which the major principal stress (σ_1) is operating in approximately WNW direction, while the intermediate stress (σ_2) operates vertically and the least principal stress (σ_3) horizontally in NNE direction respectively. This stress system indicates that the Gülpınar-Tuzla earthquake area, which is included in the central to northern Aegean Sea neotectonic province, has been experiencing a strike-slip neotectonic regime since at least early Quaternary.

In general, the geodetic slip rate throughout the NAFS ranges from 20 mm/yr to 30 mm/yr (Barka and Reilinger, 1997; McClusky et al., 2000; Reilinger et al., 2006; Dolan and Meade, 2017). However, the NAFS is divided into two major strands, namely the northern and southern strands, respectively, in the Marmara region. Accordingly the slip rate on it is also partitioned by these two strands. In most of geodetic studies, the Marmara region is taken into account as a single block or a geodetic velocity field bounded by the northern strand in the north and by the southern strand in the south (Meade et al., 2002; Aktuğ et al., 2009). They also accepted that these boundary strands consist of single fault zones such as the northerly located Kuzey Marmara-Ganos Fault Zone and the southerly located Yenice-Gönen Fault Zone, i.e., other fault zones comprising the southern strand were ignored. According to the geodetic data, the slip rate on the northern strand is faster than those on the southern strand. It ranges from 24 mm/yr to 10 mm on the northern strand, and from 12 mm/yr to 4 mm/yr on the southern strand (Meade et al., 2002; Flerit et al., 2003; Aktuğ et al., 2009; Gasperini et al., 2011; Kurt et al., 2013).

In contrast to the geodetic studies, the southern strand of the NAFS consists of multiple fault zones of dissimilar character ranging from strike-slip fault to oblique-slip normal fault (Koçyiğit, 2000, 2006, 2011, 2012). These are, from north to south, the Çan-Biga, Sarıköy-İnova, Yenice-Gönen and the Edremit fault zones on the land (Figures 1 and 3b). In the same way, the slip rate on the southern strand is also partitioned among these fault zones. Based on the morphotectonic markers (mostly offset drainage systems) the average geologic slip rates on the Çan-Biga, Sarıköy-İnova, Yenice-Gönen, and Edremit fault zones are 7.7 mm/yr, 4.6 mm/yr, 10.8 mm/yr and 7.3 mm/yr respectively. The total slip rate on the southern strand is approximately 30 mm/yr. The geologic slip rate seems to contradict with the geodetic slip rate. This can be explained in two ways: 1) the drainage systems have not been displaced by the fault zones, i.e., they followed the fault zone of weakness after they have entered into them; 2) they have been offset by the related fault zones. In our study, the second possibility was preferred. Because, the Aegean Sea and southwest Anatolia altogether move at a rate of 30-40 mm/yr on the asthenosphere in SSW direction (Barka and Reilinger, 1997). This relatively faster motion leads to internal deformation, i.e., accumulation of high elastic strain in the overlying Anatolian platelet. This high elastic strain can't be accommodated by slow slip rate along fault zones. Therefore the total slip rate on the southern strand must be faster than the abovementioned geodetic slip rates on the southern strand of the NAFS. For this reason, the central to northern Aegean Sea and its eastern coastal areas bounded by the BİFZ must be evaluated under a separate neotectonic domain.

6. Results

The central to northern Aegean Sea and its coastal areas are a new neotectonic domain characterized by prominent strike-slip faulting. For this reason, fault-bounded depressions in it are pull-apart basins of dissimilar shape and origin. Its eastern approximate boundary is the Balıkesir-İzmir Fault Zone (BİFZ) located between Lake Ulubat in the NNE and Samos Island in the SSW. This Quaternary neotectonic domain is governed by the WNW-directed operation of principal compressive stress (σ_1). The Biga Peninsula and our study area are also included in this domain shaped mostly by the southern strand of the NAFS. The total slip rate on this strand is about 30 mm/yr. But it is partitioned by four major and numerous second- and third-order fault zones to single faults. Therefore, return period of peak earthquakes with Mw 6.5 or greater than it to be sourced from major fault zones, such as the Çan-Biga, Sarıköy-İnova, Yenice-Gönen and Edremit fault zones, will be at least 400 hundred years or longer than it. However, the return periods of small earthquakes are shorter than 400 hundreds years. This was proved once more by the occurrence of the Gülpınar-Tuzla earthquake cluster.

The most active and well-known structure of the southern strand is the YGFZ. It consists of onshore Biga and the offshore Behramkale-Skyros sections. The master fault (Y-shear) of the southern strand is included in the YGFZ. The age of the YGFZ is early Quaternary (approximately 2.6 ma yr. BP), and the total right lateral strike-slip displacement accumulated on it is about 28 ± 2 km. This value implies an average uniform slip rate of 10.8 mm/yr. The Yenice-Gönen section of the master fault reactivated and caused the occurrence of the 18 March 1953 Yenice destructive earthquake and the 40 km long surface rupture. The average coseismic dextral strike-slip displacement was 4.2 m during this big earthquake (Ms = 7.4). The recurrence interval of the big earthquakes to be sourced from the southern major strand of the NAFS seems as at least 400 years based on the uniform slip rate (10.8 mm/yr) and the coseismic dextral displacement.

References

AFAD. 2017. Disaster and Emergency Management Presidency, Earthquake Catalog.

Aksoy, M. E., Meghraouil, M., Vallée, Çakır, Z. 2010. Rupture characteristics of the A. D. 1912 Mürefte (Ganos) earthquake segment of the North Anatolian fault (western Turkey). Geology 38(11), 991-994.

Aksoy, E., İnceöz, M., Kocyiğit, A. 2007. Lake Hazar basin: a negative fl ower structure on the East Anatolian fault system (EAFS), SE Turkiye. Turkish Journal of Earth Sciences 16, 319-338.

Aktuğ, B., Nocquet, J. M., Cingöz, Z., Parsons, B., Erkan, Y., England, P., Lenk, O., Gürdal, M. A., Kılıçoğlu, A., Akdeniz, H., Tekgül, A. 2009. Deformation of Western Turkey from a combination of permanent and campaign GPS data: Limits to blocklike behavior. Journal of Geophysical Research 114, B10404.

Altınok, Y., Alpar, B., Yaltırak, C., Pınar, A., Özer, N. 2012. The earthquakes and related tsunamis of October 6, 1944 and March 7, 1867; NE Aegean Sea. Natural Hazards 60, 3-25.

Ambraseys, N. N. 1988. Engineering seismology. Journal of Earthquake Engineering and Structure Dynamics 17, 1-105.

Ambraseys, N. N., Finkel, C. 1995. The Seismicity of Turkey and Adjacent Areas: A Historical Review. 1500-1800. Eren Yayıncılık, İstanbul, 240.

Ambraseys, N., Jackson, J. 1998. Faulting associated with historical and recent earthquakes in the Eastern Mediterranean. Geophysical Journal International 133, 390-406.

Barka, A. A., Kadinsky Cade, K. 1988. Strike-slip fault geometry in Turkey and its influence on earthquake activity. Tectonics 7, 66-684.

Barka, A., Reilinger, R. 1997. Active tectonics of the eastern Mediterranean region: deduced from GPS, neotectonic, and seismicity data. Annali Di Geofisica 40(3), 587-610.

Beccaletto, L., Steiner, C. 2005. Evidence of two-stage extensional tectonics from the northern edge of the Edremit graben, NW Turkey. Geodinamica Acta 18, 283-297.

Borsi, J., Ferrara, G., Innocenti, F., Mazzuoli, R. 1972. Geochronology and petrology of recent volcanics in the Eastern Aegean Sea (West Anatolia and Lesvos Island). Bulletin of Volcanology 36, 473-496.

Bozkurt, E. 1996. Metamorphism of Paleozoic schists in the Southern Menderes Massif: field, petrographic, textural and microstructural evidence. Turkish Journal of Earth Sciences 5, 105-121.

Bozkurt, E. 2004. Granitoid rocks of the southern Menderes Massif (southwestern Turkey): field evidence for Tertiary magmatism in an extensional shear zone. International Journal of Earth Sciences (Geologische Rundschau) 93, 52-71.

Bozkurt, E., Park, R. G. 1997. Evolution of a mid-Tertiary extensial shear zone in the southern Menderes Massif, Western Turkey. Bulletin De La Societe Géologique De France 168, 3-14.

Bozkurt, E., Park, R. G. 1999. The structure of the Paleozoic schists in the Southern Menderes Massif, Western Turkey: a new approach to the origin of the main Menderes metamorphism and its relation to the Lycian Nappes. Geodinamica Acta 12, 25-42.

Brunn, J. H., Graciansky, P. C., Gutnie, M., Juteau, T. H., Fevere, R., Marcous, J., Monod, O., Poisson, A. 1971. Structures majeurs et correlations stratigraphiques dans Taurides occidentals: Bulletin Geological Society of France 12, 516-556.

Çolak, S., Aksoy, E., Koçyiğit, A., İnceöz, M. 2012. Palu-Uluova strike-slip basin on the East Anatolian Fault System, Turkey: transition from paleotectonic period to neotectonic period. Turkish Journal of Earth Sciences 21(4), 547-570.

Dewey, J. F., Hempton, M. R., Kidd, W. S. F., Şaroğlu, F., Şengör, A. M C. 1986. Shortening of continental lithosphere: the neotectonics of Eastern Anatolia - a young collision zone. Coward, M.P., Ries, A.C. (Ed.). Collisional Tectonics. Geological Society, London, Special Publications 19, 3-36.

Dewey, J. F. 1988. Extensional collapse of orogens. Tectonics 7, 1123-1139.

Dolan, J. F., Meade, B. J., 2017. A comparison of geodetic and geologic rates prior to large strike-slip earthquakes: a diversity of earthquake-cycle behaviors? Geochemistry, Geophysics, Geosystems 18.

Emre, T., Sözbilir, H. 2005. Küçük Menderes Grabeni doğu ucundaki andezitlerin (Başova-Kiraz/İzmir) jeolojisi, petrografisi ve jeokimyası. Bulletin of the Mineral Research and Exploration 131, 1-19.

Emre, Ö., Doğan, A. 2010. 1/250000 ölçekli Türkiye aktif fay haritaları serisi, Ayvalık (NJ 35-2) paftası (Seri No: 4). Maden Tetkik ve Arama Genel Müdürlüğü (MTA), Ankara.

EMSC. 2020. European-Mediterranean Seismological Centre.

Ercan, T., Satır, M., Kreuzer, H., Türkecan, A., Günay, E., Çevikbaş, A., Ateş, M., Can, B. 1985. Batı Anadolu Senozoyik volkanitlerine ait yeni kimyasal, izotopik ve radyometrik verilerin yorumu. Geological Society of Turkey Bulletin 28, 121-136 (In Turkish with English abstract).

Ercan, T., Fujitani, T., Madsuda, J. I., Notsu, K., Tokel, S., Ui, T. 1990. Doğu ve Güneydoğu Anadolu Neojen-Kuvaterner volkaniklerine ilişkin yeni jeokimyasal, radiometrik ve izotopik verilerin yorumu. Bulletin of the Mineral Research and Exploration 110, 143-164.

Ercan, T., Satır, M., Dora, A., Sarıkoğlu, E., Yıldırım, T., Adis, C., Walter, H. J., Özbayrak, İ. H. 1995. Biga Yarımadası, Gökçeada, Bozcaada ve Tavşan Adaları'ndaki Tersiyer yaşlı volkanitlerin petrolojisi ve bölgesel yayılımı. Bulletin of the Mineral Research and Exploration 117, 55-86.

Erkül, F., Helvacı, C., Sözbilir, H. 2005*a*. Stratigraphy and geochronology of the Early Miocene volcanic units in the Bigadiç borate basin, western Turkey. Turkish Journal of Earth Sciences 14, 227-253.

Erkül, F., Helvacı, C., Sözbilir, H. 2005*b*. Evidence for two episodes of volcanism in the Bigadic¸ borate basin and tectonic implications for western Turkey. Geological Journal 40, 545-570.

Eryılmaz, M., Yücesoy Eryılmaz, F. 1999. Ege Denizi'nin tektonik yapısı. 52. Türkiye Jeoloji Kurultayı Bildiriler Kitabı, 10-12 Mayıs. Ankara, 358-365.

Flerit, F., Armijo, R., King, G. C. P., Meyer, B., Barka, A. 2003. Slip partitioning in the Sea of Marmara pull-apart determined from GPS velocity vectors. Geophysical Journal International 154**,** 1-7.

Gasperini, L., A. Polonia, Çağatay, N., Bortoluzzi, G., Ferrante, V. 2011. Geological slip rates along the North Anatolian Fault in the Marmara region. Tectonics 30, TC1010.

GCMT. 2017. Global Centroid Moment Tensor Catalog. Harvard University, USA.

GCMT. 2020. Global Centroid Moment Tensor Catalog. Harvard University, USA.

Genç, Ş. C. 1998. Evolution of the Bayramiçi magmatic complex. Journal of Volcanology and Geothermal Research 85, 233-249.

Gevrek, A. İ., Şener M, Ercan, T. 1985. Çanakkale-Tuzla jeotermal alanının hidrotermal alterasyon etüdü ve volkanik kayaçların petrolojisi. Bulletin of the Mineral Research and Exploration 103-104, 82-103.

GFZ. 2017. German Research Centre for Geosciences.

Glodny, J., Hetzel, R. 2007. Precise U–Pb ages of syn-extensional Miocene intrusions in the central Menderes Massif, western Turkey. Geological Magazine 144, 235–246.

Güney, A., Yılmaz, Y., Demirbağ, E., Ecevitoğlu, B., Arzuman, S., Kuşçu, İ. 2001. Reflection seismic study across the continental shelf of Baba Burnu promontory of Biga Peninsula, Northwest Turkey. Marine Geology 176, 75-85.

Gürer, Ö. F., Sangu, E., Özburan, M., Gürbüz, A., Gürer, A., Sinir, H. 2016. Plio-Quaternary kinematic development and paleostress pattern of the Edremit Basin, western Turkey. Tectonophysics 679, 199-210.

Harris, N. B. W., Pearce, J. A., Tindle, A. G. 1986. Geochemical Characteristic of Collision-Zone Magmatism. Coward, M. P., Reis, A. C. (Ed.). In Collision Tectonics. Geological Society of London, Special Publication 19, 67-81.

Harvard. 2017. GCMT catalogue.

Hempton, M. R. 1987. Constraints on Arabian plate motion and extensional history of Red Sea. Tectonics 6, 687-705.

Herece, E. 1985. The fault trace of 1953 Yenice Gönen Earthquake and Some Examples of Recent Tectonic Events in the Biga Peninsula of Northwest Turkey. MSc Thesis, Pennsylvania State University, 143, US (unpublished).

Herece, E. 1990. 1953 Yenice-Gönen deprem kırığı ve Kuzey Anadolu fay sisteminin Biga Yarımadası'ndaki uzantıları. Bulletin of the Mineral Research and Exploration 111, 47-59.

Innocenti, F., Pısa, R., Mazzuoli, C., Pasquare, G., Serri, G., Villari, L. 1980. Geology of the volcanic area north of Lake Van (Turkey). Geologische Rundschau 69, 292-322.

Kalafat, D., Güneş, Y., Kekovalı, K., Kara, M., Deniz, P., Yılmazer, M. 2011. Türkiye için 1900 yılından bu yana revize edilmiş ve genişletilmiş deprem kataloğu (M≥4.0). Boğaziçi University Publications 1049, 640.

Karacık, Z., Yılmaz, Y. 1998. Geology of ignimbrites and the associated volcano-plutonic complex of the Ezine area, Northwestern Anatolia. Journal of Volcanology and Geothermal Research 85, 251-264.

Karakaisis, G. F., Papazachos, C. B., Scordilis, E. M. 2010. Seismic sources and main seismic faults in the Aegean and surrounding area. Bulletin of the Geological Society of Greece 43(4), 2026-2042.

Katsikatsos, G., Mataragas, D., Migiros, G., Triandafillou, E. 1982. Geological study of Lesbos Island. IGME, Special Report No: 92.

Ketin, I., Roesly, F. 1953. Makroseismische untersuchungen über das nord-westanatolische Beben vom 18 Marz 1953. Eclogae Geologicae Helvetiae 46(2), 187-208.

Kiratzi, A. A., Wagner, G. S., Langston, C. A. 1991. Source parameters of some large earthquakes in Northern Aegean determined by body waveform inversion. Pure and Applied Geophysics 135, 515-527.

Koçyiğit, A. 1983. Hoyran gölü (Isparta Büklümü) dolayının tektoniği. Geological Society of Turkey Bulletin 26, 1-10 (In Turkish with English abstract).

Koçyiğit, A. 1984. Güneybatı Türkiye ve yakın dolayında levha içi yeni tektonik gelişim. Geological Society of Turkey Bulletin 27, 1-16 (In Turkish with English abstract).

Koçyiğit, A. 2000. Güneybatı Türkiye'nin depremselliği. Symposium on the Seismicity of Western Turkey (Badsem) 2000 Abstracts and Proceedings 30, 2000, 30-38 (In Turkish with English abstract).

Koçyiğit, A. 2005. Denizli Graben-Horst System and the eastern limit of the West Anatolian continental extension: basin fill, structure, deformational mode, throw amount and episodic evolutionary history, SW Turkey. Geodinamica Acta 18, 167-208.

Koçyiğit, A. 2006. Çan kömür havzasının jeolojik yapısı, yapısal analizi ve fayların kazılara etkisi. ODTÜ, Mühendislik Fakültesi, Jeoloji Mühendisliği Bölümü, Aktif Tektonik ve Deprem Araştırma Laboratuvarı, Proje No. 2006-03-05-2-00-13, 20 (unpublished).

Koçyiğit, A. 2011. Gönen (Balıkesir) ruhsat sahalarının aktif tektonik yönden değerlendirilmesi. ODTÜ, Jeoloji Mühendisliği Bölümü, Aktif Tektonik ve Deprem Araştırmaları Laboratuvarı, Proje No: 11-03-09-1-0018, 43 (unpublished).

Koçyiğit, A. 2012. Saruhanlı (Manisa) ruhsat sahaları jeotermal potansiyelinin Aktif tektonik yönden değerlendirilmesi. Middle East Technical University, Enginering Faculty, Department of Geological Engineering, Active Tectonic and Earthquake Research Laboratory, Report, 31 (unpublished).

Koçyiğit, A. 2013. New field and seismic data about the intraplate strike-slip deformation in Van region, East Anatolian plateau, E. Turkey. Journal of Asian Earth Sciences 62, 586-605.

Koçyiğit, A. 2020. İzmir ili Seferihisar ilçesi 2107 nolu jeotermal işletme ruhsatı ile 1586 nolu arama ruhsatlarının bulunduğu sahanın jeolojik çalışması ve toplanan verilerin değerlendirilmesiyle igili teknik rapor. Middle East Technical University, Department of Geological Engineering, Active Tectonics and Earthquake Research Labaratory, 81, Ankara.

Koçyiğit, A., Beyhan, A. 1998. A new intracontinental transcurrent structure: the Central Anatolian Fault Zone, Turkey. Tectonophysics 284, 317-336.

Koçyiğit, A., Özacar, A. 2003. Extensional neotectonic Regime through the NE edge of the outer Isparta angle, SW Turkey: new field and seismic data. Turkish Journal of Earth Sciences 12, 67-90.

Koçyiğit, A., Canoğlu, M. C. 2017. Neotectonics and seismicity of Erzurum pull-apart basin, East Turkey. Russian Geology and Geophysics 58, 99-122.

Koçyiğit, A., Yusufoğlu, H., Bozkurt, E. 1999. Evidence from the Gediz graben for episodic two-stage extension in Western Turkey. Journal of the Geological Society of London 156, 605-616.

Koçyiğit A. Ünay, E., Saraç, G. 2000. Episodic graben formation and extensional neotectonic regime in west Central Anatolia and the Isparta Angle: a key study in the Akşehir-Afyon graben, Turkey. Geological Society of London, Special Publications 173, 405-421.

Koçyiğit, A., Yılmaz, A., Adamia, S., Kuloshvili, S. 2001. Neotectonic of East Anatolian Plateau (Turkey) and Lesser Caucasus: implication for transition from thrusting to strike-slip faulting. Geodinamica Acta 14, 177-195.

Koukouvelas, I. K., Aydın, A. 2002. Fault structure and related basins of the North Aegean Sea. Tectonics 21(5), 1046.

Kurt, H., Sorlien, C. C., Seeber, L., Steckler, M. S., Shillington, D. J., Çifçi, G., Cormier, M. H., Dessa, X., Atgin, O., Dondurur, D., Demirbağ, E., Okay, S., İmren, C., Gürçay, S., Carton, H. 2013. Steady late quaternary slip rate on the Çinarcik section of the North Anatolian fault near Istanbul, Turkey. Geophysical Research Letter 40, 4555-4559.

Kurtuluş, C., Doğan, B., Sertçelik, F., Canbay, M., Küçük, H. M. 2009. Determination of the tectonic evolution of the Edremit Gulf based on seismic reflection studies. Marine Geophysical Research 30, 121-134.

Kürçer, A. 2006. Neotectonic features of the vicinity of Yenice - Gönen and paleoseismology of March 18, 1953 (Mw: 7.2) Yenice - Gönen Earthquake Fault (NW Turkey). MSc Thesis, Çanakkale Onsekiz Mart University.

Kürçer, A., Chatzipetros, A., Tutkun, S. Z., Pavlides, S., Ateş, Ö., Valkaniotis, S. 2008. The Yenice-Gönen active fault (NW Turkey): active tectonics and palaeoseismology. Tectonophysics 453, 263-275.

Kürçer, A., Yalçın, H., Gülen, L., Kalafat, D. 2015. 8 January 2013 Mw = 5.7 North Aegean Sea earthquake and its seismotectonic significance. Geodinamica Acta 27, 175-188.

Kürçer, A., Özalp, S., Özdemir, E., Uygun Güldoğan, Ç., Duman, T. Y., 2019. Active tectonic and paleoseismologic characteristics of the Yenice-Gönen Fault, NW Turkey, in light of the 18 March 1953 Yenice-Gönen Earthquake (Ms=7.2). Bulletin of the Mineral Research and Exploration 159, 29-62.

McClusky, S., Balassanian, S., Barka, A., Demir, C., Ergintav, S., Georgiev, I., Gürkan, O., Hamburger, M., Hurst, K., Kahle, G. H., Kastens, K., Kekelidze, G., King, R., Kotzev, V., Lenk, O., Mahmoud, S., Mishin, A., Nadariya, M., Ouzounis, A., Paradissis, D., Peter, Y., Prilepin, M., Reilinger, R., Sanli, I., Seeger, H., Tealeb, A., Toksöz, M. N., Veis, G. 2000. Global positioning system constrains on plate kinematics and dynamics in the Eastern Mediterranean and Caucasus. Journal of Geophysical Research B3(105), 5695-5719.

Meade, B. J., Hager, B. H., McClusky, S., Reilinger, R. E., Ergintav, S., Lenk, O.,Özener, H. 2002. Estimates of seismic potential in the Marmara Sea region from block models of secular deformation constrained by global positioning system measurements. Bulletin of the Seismomlogical Society of America 92, 208-215.

Okay, A. 1986. High-pressure-low-temperature metamorphic rocks of Turkey. Geological Society of America Memoir 164, 333-347.

Okay, A. I., Siyako, M., Bürkan, K. A. 1990. Geology and tectonic evolution of the Biga Peninsula. Turkish Association of Petroleum Geologists Bulletin 2, 83-121.

Özgül, N. 1984. Torosların bazı temel jeoloji özellikleri. Bulletin of the Geological Society of Turkey 19, 65-78 (In Turkish with English abstract).

Papazachos, B. C. 2003. The earthquakes of Greece. Ziti Publications, Thessaloniki, 286.

Papazachos, B. C., Kiratzi, A., Hatzidimitriou, P., Rocca, A. 1984. Seismic faults in the Aegean area. Tectonophysics 106, 71-85.

Papazachos, B. C., Kiratzi, A., Papadimitriou, E. 1991. Regional focal mechanisms for earthquakes in the Aegean area. Pure Applied Geophysics 136, 405-420.

Papazachos, B. C., Papadimitriou, E. E., Kiratzi, A., Papazachos, B. C. 1998. Fault plane solutions in the Aegean Sea and the surrounding area and their tectonic implication. Bollettino Di Geofisica Teorica Ed Applicata 39, 3.

Pınar, N., Lahn, E. 1952. Türkiye depremleri izahlı kataloğu. Bayındırlık ve İskân Bakanlığı, İmar Reisliği Publications 6, 36, Ankara (in Turkish).

Pinet, B., Colletta, B. 1990. Probing into extensional sedimentary basins: comparison of recent data and derivation of tentative models. Tectonophysics 173, 185-197.

Reilinger, R., McClusky, S., Vernant, P., Lawrence, S., Ergintav, S., Çakmak, R., Karam, G. 2006. GPS constraints on continental deformation in the Africa-Arabia-Eurasia continental collision zone and implications for the dynamics of plate interactions. Journal of Geophysical Research 111(B05411).

Saka, K. 1979. Edremit Körfezi ve civarı Neojeni'nin jeolojisi ve hidrokarbon olanakları. Türkiye Petrolleri Anonim Ortaklığı, Rapor No: 1342, 17.

Seyitoğlu, G., Scott, B. C. 1991. Late Cenozoic crustal extension and basin formation in West Turkey. Geological Magazine 128, 155-166.

Siyako, M., Bürkan, K. A., Okay, A. İ. 1989. Tertiary geology and hydrocarbon potential of the Biga and Gelibolu peninsulas. Bulletin of Turkish Petroleum Geologists 1, 183-199.

Sözbilir, H. 2005. Oligo-Miocene extension in the Lycian orogen: Evidence from the Lycian molasse basin, Southwestern Turkey. Geodinamica Acta 18, 255-282.

Sözbilir, H., İnci, U., Erkül, F., Sümer, Ö. 2013. An active intermitten transform zone accommodating N-S extension in Western Anatolia and its relation to the North Anatolian Fault System International Workshop on the North Anatolian and Dead Sea Fault Systems: Recent Progress in Tectonics and Paleoseismology, and Field Training Course in Paleoseismology, Ankara.

Sözbilir, H., Özkaymak, Ç., Uzel, B., Sümer, Ö., Eski, S., Tepe, Ç. 2016. Palaeoseismology of the Havran-Balıkesir Fault Zone: evidence for past earthquakes in the strike-slip-dominated contractional deformation along the southern branches of the North Anatolian fault in northwest Turkey. Geodinamica Acta 28, 254-272.

Şahin, S. Y., Örgün, Y., Güngör, Y., Göker, A. F., Gültekin, A. H., Karacık, Z. 2010. Mineral and whole-rock geochemistry of the Kestanbol Granitoid (Ezine-Çanakkale) and its mafic mikrogranular enclaves in Northwestern Anatolia: evidence of felsic and mafic magma interaction. Turkish Journal of Earth Sciences 19, 101-122.

Şamilgil, E. 1983. Geothermal energy fields of Canakkale and Tuzla drillings. Bulletin of Geology Congress Turkey 4, 147-159.

Şaroğlu, F., Boray, A., Emre, Ö. 1987. Türkiye'nin aktif fayları. General Directorate of Mineral Research and Exploration, Report No: 8643, 394, Ankara (unpublished).

Şaroğlu, F., Yılmaz, Y., 1986. Doğu Anadolu'da neotektonik dönemdeki jeolojik evrim ve havza modelleri. Bulletin of the Mineral Research and Exploration 107, 73-94.

Şengör, A. M. C. 1980. Türkiye'nin neotektoniğinin esasları. Türkiye Jeoloji Kurumu, Conference Series 2, Ankara, 40.

Şengör, A. M. C., Kidd, W. S. F. 1979. Post-collisional tectonics of the Turkish-Iranian plateau and a comparison with Tibet. Tectonophysics 55, 361-376.

Şengör, A. M. C., Yılmaz, Y. 1981. Tethyan evolution of Turkey: a plate tectonic approach. Tectonophysics 75, 181-241.

Şengör, A. M. C., Satır, M., Akkök, R. 1984. Timing of tectonic events in the Menderes Massif, western Turkey: implications for tectonic evolution and evidence for Pan-African basement in Turkey. Tectonics 3, 693-707.

Tan, O. M., Tapırdamaz, C., Yörük, A. 2008. The earthquake catalogues for Turkey. Turkish Journal of Earth Sciences 17, 405-418.

Taymaz, T., Eyidoğan, H., Jackson, J. 1991. Source parameters of large earthquakes in the East Anatolian Fault Zone (Turkey). Geophysical Journal International 106, 537-550.

Uzel, B., Sözbilir, H. 2008. A first record of a strike-slip basin in Western Anatolia and its tectonic implication: The Cumaovası basin. Turkish Journal of Earth Sciences 17, 559-591.

Wells, D. L., Coppersmith, S. R. 1994. New empirical relationships among magnitude rupture length, rupture width, rupture area and surface displacement. Bulletin of the Seismological Society of America 84, 974-1002.

Wilson, M., Bianchini, G. 1999. Tertiary-Quaternary magmatism within the Mediterranean and surrounding regions. Geological Society of London, Special Publications 156, 141-166.

Yaltırak, C. 2003. Edremit Körfezi ve kuzeyinin jeodinamik evrimi. PhD Thesis, İTÜ Eurasia Institute of Earth Sciences, 242.

Yaltırak, C., İşler, E. B., Aksu, A. E., Hiscott, R. H. 2013. Evolution of the Bababurnu Basin and shelf of the Biga Peninsula: Western extension of the middle strand of the North Anatolian Fault Zone, Northeast Aegean Sea, Turkey. Journal of Asian Earth Sciences 57, 103-119.

Yazman, M. 1996. Batı Anadolu Grabenleri Jeolojisi Gezisi (Field excursion on the geology of western Anatolian grabens). Türkiye Petrolleri Anonim Ortaklığı, Saha Raporu No: 13-20 August, 77.

Yılmaz, Y., Karacık, Z. 2001. Geology of the northern side of the Gulf of Edremit and its tectonic significance for the development of the Aegean grabens. Bozkurt, E. (Ed.). Neotectonics of Turkey. Geodinamica Acta 14, 31-43.

Yılmaz, Y., Şaroğlu, F., Güner, Y. 1987. Initiation of the neomagmatism in East Anatolia. Tectonophysics 134, 177-194.

Yılmaz, Y., Genç, S.C., Gürer, F., Bozcu, M., Yılmaz, K., Karacık, Z., Altunkaynak, S., Elmas, A. 2000. When did the Western Anatolian grabens begin to develop? Geological Society of London, Special Publications 173, 353-384.